arXiv:1607.01883v4 [cs.RO] 4 Feb 2017

Sampling-based Incremental Information Gathering with Applications to Robotic Exploration and Environmental Monitoring*

Maani Ghaffari Jadidi† Jaime Valls Miro† Gamini Dissanayake†

February 7, 2017

Abstract

In this article, we propose a sampling-based motion planning algorithm equipped with an information-theoretic convergence criterion for incremental informative motion planning. The proposed approach allows dense map representations and incorporates the full state uncertainty into the planning process. The problem is formulated as a maximization problem with a budget constraint. Our approach is built on rapidly-exploring information gathering algorithms and benefits from advantages of sampling-based optimal motion planning algorithms. We propose two information functions and their variants for fast and online computations. We prove an information-theoretic convergence for the entire exploration and information gathering mission based on the least upper bound of the average map entropy. The convergence criterion gives rise to a natural automatic stopping criterion for information-driven motion control. We demonstrate the performance of the proposed algorithms using three scenarios: comparison of the proposed information functions and sensor configuration selection, robotic exploration in unknown environments, and a wireless signal strength monitoring task in a lake from a publicly available dataset collected using an autonomous surface vehicle.

*Working paper. mani.ghaffari@gmail.com – http://maanighaffari.com
†Centre for Autonomous Systems (CAS), University of Technology Sydney.

Contents

1 Introduction **3**

2 Related work **4**

3 Preliminaries **5**

3.1 Mathematical notation . . . 5

3.2 Probability Theory . . . 6

3.3 Information Theory . . . 6

3.4 Submodular functions . . . 8

3.5 Gaussian Processes . . . 8

3.5.1 Covariance Function . . . 9

3.5.2 Useful Kernels . . . 9

4 Problem Statement **10**

4.1 Incremental Informative Motion Planning . . . 12

4.2 RIG Algorithms . . . 12

4.3 System Dynamics . . . 14

5 IIG: Incrementally-exploring Information Gathering **14**

6 Information Functions Algorithms **16**

6.1 Mutual Information . . . 17

6.2 GP Variance Reduction . . . 20

6.3 Uncertain GP Variance Reduction . . . 22

7 Path Extraction and Selection **23**

8 Information-theoretic Robotic Exploration **25**

9 Results and Discussion **26**

9.1 Experiments Setup . . . 28

9.2 Comparison of Information Functions . . . 28

9.3 Robotic Exploration in Unknown Environments . . . 34

9.4 Lake Monitoring Experiment . . . 35

9.5 Limitations and Observations . . . 38

10 Conclusion and Future Work **40**

1 Introduction

Exploration in unknown environments is a major challenge for an autonomous robot and has numerous present and emerging applications from search and rescue operations to space exploration programs. While exploring an unknown environment, the robot is often tasked to monitor a quantity of interest through a cost or an information quality measure (Dhariwal et al. 2004; Singh et al. 2010; Marchant and Ramos 2012; Dunbabin and Marques 2012; Lan and Schwager 2013; Yu et al. 2015). Robotic exploration algorithms usually rely on geometric frontiers (Yamauchi 1997; Ström et al. 2015) or visual targets (Kim and Eustice 2015) as goals to solve the planning problem using geometric/information gain-based *greedy* action selection or planning for a limited horizon. The main drawback of such techniques is that a set of targets constrains the planner search space to the paths that start from the current robot pose to targets. In contrast, a more general class of robotic navigation problem known as robotic information gathering (Singh et al. 2009; Binney and Sukhatme 2012; Binney et al. 2013), and in particular the Rapidly-exploring Information Gathering (RIG) (Hollinger and Sukhatme 2013, 2014) concept exploits a sampling-based planning strategy to calculate the cost and information gain while searching for traversable paths. This approach differs from classic path planning problems as there is no goal to be found. Therefore, a solely information-driven robot control can be formulated. Another important advantage of RIG methods is their *multi-horizon planning* nature through representing the environment by an incrementally built graph that considers both the information gain and cost.

Rapidly-exploring information gathering algorithms are suitable for non-myopic robotic exploration techniques. However, the developed methods are not online, the information function calculation is often a bottleneck, and they do not offer an automated convergence criterion, i.e. they are *anytime* [1]. To be able to employ RIG for online navigation tasks, we propose an IIG algorithm built on the RIG. In particular, the following developments are performed:

(i) We allow the full state including the robot pose and a dense map to be partially observable.

(ii) We develop a convergence criterion based on relative information contribution. This convergence criterion is a necessary step for incremental planning as the robot needs to execute planned actions autonomously.

(iii) We propose two information functions (five including their variants) that can approximate the information gain for online applications. The algorithmic implementation of the proposed functions is also provided.

(iv) We develop a heuristic algorithm to extract the most informative trajectories.

(v) We prove an information-theoretic automatic stopping criterion for the entire mission based on the least upper bound of the average map entropy.

[1] Being anytime is typically a good feature, but we are interested in knowing when the algorithm converges.

(vi) We provide results in batch and incremental experiments as well as in publicly available robotic datasets and discuss potential applications of the developed algorithms.

This article is organized as follows. In the next section, the related work is discussed. Section 3 includes required preliminaries. In Section 4, we present the problem definition and make the difference between RIG and IIG algorithms clear. We also explain RIG algorithms to establish the required basis. In Section 5, we present the novel IIG algorithm. In Section 6, we discuss the proposed information functions to approximate the information quality of nodes and trajectories. In Section 7, the problem of path extraction and selection is explained, and a heuristic algorithm is proposed to solve the problem. Section 8 presents the proof for an information-theoretic automatic stopping criterion for exploration and information gathering missions. In Section 9, we present results from the comparison of the proposed information functions, exploration experiments including comparison with relevant techniques in the literature, a lake monitoring scenario, and discuss the limitations and possible extension of this work. Finally, Section 10 concludes the article.

2 Related work

Motion planning algorithms (Latombe 1991; LaValle 2006) construct a broad area of research in the robotic community. Here, we briefly summarize some of the fundamental and most relevant works related to this article. Under the presence of uncertainty, where the state is not fully observable, measurements and actions are stochastic. The sequential decision-making under uncertainty, in the most general form, can be formulated as a Partially Observable Markov Decision Processes (POMDP) or optimal control with imperfect state information (Astrom 1965; Smallwood and Sondik 1973; Bertsekas 1995; Kaelbling et al. 1998). Unfortunately, when the problem is formulated using a dense belief representation, a general purpose POMDP solver is not a practical choice (Binney et al. 2013).

The sampling-based motion planning algorithms (Horsch et al. 1994; Kavraki et al. 1996; LaValle and Kuffner 2001; Bry and Roy 2011; Karaman and Frazzoli 2011; Lan and Schwager 2013) have proven successful applications in robotics. An interesting case is where the environment is fully observable (known map) and the objective is to make sequential decisions under motion and measurement uncertainty. This problem is also known as *active localization*; for a recent technique to solve such a problem see Aghamohammadi et al. (2014, and references therein). A closely related term that is used in the literature is *belief space planning* (Kurniawati et al. 2008; Huynh and Roy 2009; Prentice and Roy 2009; Platt Jr et al. 2010; Kurniawati et al. 2011; Van Den Berg et al. 2011; Bry and Roy 2011; Valencia et al. 2013). In this series of works, the assumption of a known map can be relaxed and the environment is often represented using a set of features. The objective is to find a trajectory that minimizes the state uncertainty (the total cost) with respect to a fixed or variable (and bounded) planning horizon that can be set according to the *budget* (Indelman et al. 2015).

However, in the problem we study in this article, the state variables consist of the robot trajectory

and a dense map of the environment. Another approach to study the problem of robotic navigation under uncertainty, is known as informative motion planning or robotic information gathering (Singh et al. 2009; Levine 2010; Binney and Sukhatme 2012; Binney et al. 2013; Hollinger and Sukhatme 2013, 2014). Rapidly-exploring information gathering (Hollinger and Sukhatme 2014), is a technique that solves the problem of informative motion planning using incremental sampling from the workspace and by *partial ordering* of nodes builds a graph that contains informative trajectories. In this article, we develop this technique by considering the robot pose and the map being both partially observable. We also develop an information-theoretic criterion for the convergence of the search which allows us to perform online robotic exploration experiments in an unknown environment. The Rapidly-exploring Adaptive Search and Classification (ReASC) (Hollinger 2015) also improves on the Rapidly-exploring information gathering by allowing for real-time optimization of search and classification objective functions. However, ReASC considers discrete target locations and, similar to Platt Jr et al. (2010), resorts to the maximum likelihood assumption for future observations.

In particular, the main features of this work that differentiate the present approach from the literature mentioned above can be summarized as follows.

(i) We allow for dense belief representations. Therefore, we incorporate full state uncertainty, i.e. the robot pose and the map, into the planning process. As a result, the robot behavior has a strong correlation with its perception uncertainty.

(ii) We take into account all possible future observations and do not resort to maximum likelihood assumptions. Therefore, in expectation, the randomness of future observations is addressed.

(iii) We take into account both cost and information gain in which are included a measure of distance, motion uncertainty, and the sensing information gain. Therefore, the planning algorithm runs with respect to available sensing resources, and acting limitations.

(iv) We interpret an information-theoretic notion of planning horizon which brings more flexibility for managing the convergence of the algorithm. This novel notion makes the planner an infinite-horizon planning technique and provides a general framework for robotic exploration.

3 Preliminaries

In this section, we briefly explain the mathematical notation and required preliminaries throughout this article.

3.1 Mathematical notation

In the present article probabilities and probability densities are not distinguished in general. Matrices are capitalized in bold, such as in $\boldsymbol{X}$, and vectors are in lower case bold type, such as in $\boldsymbol{x}$. Vectors are

column-wise and $1:n$ means integers from 1 to n. The Euclidean norm is shown by $\|\cdot\|$. $|\boldsymbol{X}|$ denotes the determinant of matrix $\boldsymbol{X}$. For the sake of compactness, random variables, such as X, and their realizations, x, are sometimes denoted interchangeably where it is evident from context. $x^{[i]}$ denotes a reference to the i-th element of the variable. An alphabet such as $\mathcal{X}$ denotes a set. A subscript asterisk, such as in $\boldsymbol{x}_*$, indicates a reference to a test set quantity. The n-by-n identity matrix is denoted by $\boldsymbol{I}_n$. Finally, $\mathbb{E}[\cdot]$, and $\mathbb{V}[\cdot]$ denote the expected value, variance of a random variable, respectively.

3.2 Probability Theory

Let X be a random variable that maps the sample space Ω (set of all possible outcomes) to the state space $\mathcal{X}$. Let $p(X = x) \geq 0$ be probability of the random variable X taking a specific value x. Let Y be another random variable, the joint distribution of X and Y is $p(x, y) = p(X = x \text{ and } Y = y)$ and if X and Y are independent then $p(x, y) = p(x)p(y)$. The conditional probability of X given another random variable Y is defined as $p(x|y) = \frac{p(x,y)}{p(y)}$ where $p(y) > 0$. Given the joint distribution of X and Y , the marginalization rule states that the marginal distribution of X can be computed by summing (integration) over Y. The law of total probability is its variant which uses the conditional probability definition and can be written as $p(x) = \sum_{y\in\mathcal{Y}} p(x, y) = \sum_{y\in\mathcal{Y}} p(x|y)p(y)$, and for continuous random variables is $p(x) = \int_{y\in\mathcal{Y}} p(x, y)dy = \int_{y\in\mathcal{Y}} p(x|y)p(y)dy$. Given three random variables X, Y, and Z, Bayes rule relates the prior probability distribution $p(x|z)$ and the likelihood function $p(y|x, z)$, and is $p(x|y, z) = \frac{p(y|x,z)p(x|z)}{p(y|z)}$. The term $p(x|y, z)$ is called the posterior probability distribution over X. The expected value of the random variable X is $\mathbb{E}[X] = \int_\Omega X dp = \int_\mathcal{X} xp(x)dx$ and if X is discrete $\mathbb{E}[X] = \sum_\mathcal{X} xp(x)$.

Lemma 1 (Marginalization property of normal distribution (Von Mises 1964))**.** *Let $\boldsymbol{x}$ and $\boldsymbol{y}$ be jointly Gaussian random vectors*

$$\begin{bmatrix}\boldsymbol{x}\\ \boldsymbol{y}\end{bmatrix} \sim \mathcal{N}(\begin{bmatrix}\boldsymbol{\mu}_x\\ \boldsymbol{\mu}_y\end{bmatrix}, \begin{bmatrix}\boldsymbol{A} & \boldsymbol{C}\\ \boldsymbol{C}^T & \boldsymbol{B}\end{bmatrix}) \tag{1}$$

then the marginal distribution of $\boldsymbol{x}$ is

$$\boldsymbol{x} \sim \mathcal{N}(\boldsymbol{\mu}_x, \boldsymbol{A}) \tag{2}$$

3.3 Information Theory

Entropy is a measure of the uncertainty of a random variable (Cover and Thomas 1991). The entropy $H(X)$ of a discrete random variable X is defined as $H(X) = \mathbb{E}_{p(x)}[\log \frac{1}{p(x)}] = -\sum_\mathcal{X} p(x) \log p(x)$. The joint entropy $H(X, Y)$ of discrete random variables X and Y with a joint distribution $p(x, y)$ is defined as $H(X, Y) = -\sum_{x\in\mathcal{X}} \sum_{y\in\mathcal{Y}} p(x, y) \log p(x, y)$. The chain rule implies that $H(X, Y) = H(X) + H(Y|X) = H(Y) + H(X|Y)$ where $H(X|Y)$ is the conditional entropy and is defined as $H(Y|X) = -\sum_{x\in\mathcal{X}} \sum_{y\in\mathcal{Y}} p(x, y) \log p(y|x)$.

Theorem 1 (Chain rule for entropy). *Let $X_1, X_2, ..., X_n$ be drawn according to $p(x_1, x_2, ..., x_n)$. Then*

$$H(X_1, X_2, ..., X_n) = \sum_{i=1}^{n} H(X_i | X_{i-1}, ..., X_1) \tag{3}$$

Proof. Please refer to Cover and Thomas (1991) for the proof. □

The relative entropy or Kullback-Leibler Divergence (KLD) is a measure of distance between two distributions $p(x)$ and $q(x)$. It is defined as $D(p||q) = \mathbb{E}_{p(x)}[\log \frac{p(x)}{q(x)}]$.

Theorem 2 (Information inequality). *Let X be a discrete random variable. Let $p(x)$ and $q(x)$ be two probability mass functions. Then*

$$D(p||q) \geq 0 \tag{4}$$

with equality if and only if $p(x) = q(x)\ \forall\ x$.

Proof. Please refer to Cover and Thomas (1991) for the proof. □

The mutual information (MI) $I(X;Y)$ is the reduction in the uncertainty of one random variable due to the knowledge of the other. The mutual information is non-negative and can be written as $I(X;Y) = D(p(x,y)||p(x)p(y)) = \mathbb{E}_{p(x,y)}[\log \frac{p(x,y)}{p(x)p(y)}]$ and $I(X;Y) = H(X) - H(X|Y)$.

Corollary 3 (Nonnegativity of mutual information). *For any two random variables X and Y,*

$$I(X;Y) \geq 0 \tag{5}$$

with equality if and only if X and Y are independent.

Proof. $I(X;Y) = D(p(x,y)||p(x)p(y)) \geq 0$, with equality if and only if $p(x,y) = p(x)p(y)$. □

Some immediate consequences of the provided definitions are as follows.

Lemma 2. *For any discrete random variable X, we have $H(X) \geq 0$.*

Proof. $0 \leq p(x) \leq 1$ implies that $\log \frac{1}{p(x)} \geq 0$. □

Theorem 4 (Conditioning reduces entropy). *For any two random variables X and Y,*

$$H(X|Y) \leq H(X) \tag{6}$$

with equality if and only if X and Y are independent.

Proof. $0 \leq I(X;Y) = H(X) - H(X|Y)$. □

We now define the equivalent of the functions mentioned above for probability density functions. Let X be a continuous random variable whose support set is $\mathcal{S}$. Let $p(x)$ be the probability density function for X. The differential entropy $h(X)$ of X is defined as $h(X) = -\int_{\mathcal{S}} p(x)\log p(x)dx$. Let X and Y be continuous random variables that have a joint probability density function $p(x,y)$. The conditional differential entropy $h(X|Y)$ is defined as $h(X|Y) = -\int p(x,y)\log p(x|y)dxdy$. The relative entropy (KLD) between two probability density functions p and q is defined as $D(p\|q) = \int p\log\frac{p}{q}$. The mutual information $I(X;Y)$ between two continuous random variables X and Y with joint probability density function $p(x,y)$ is defined as $I(X;Y) = \int p(x,y)\log\frac{p(x,y)}{p(x)p(y)}dxdy$.

3.4 Submodular functions

A set function f is said to be *submodular* if $\forall\mathcal{A}\subseteq\mathcal{B}\subseteq\mathcal{S}$ and $\forall s \in \mathcal{S}\backslash\mathcal{B}$, then $f(\mathcal{A}\cup s) - f(\mathcal{A}) \geq f(\mathcal{B}\cup s) - f(\mathcal{B})$. Intuitively, this can be explained as: by adding observations to a smaller set, we gain more information. The function f has diminishing return. It is *normalized* if $f(\varnothing) = 0$ and it is *monotone* if $f(\mathcal{A}) \leq f(\mathcal{B})$. The mutual information is normalized, approximately monotone, and submodular (Krause et al. 2008).

3.5 Gaussian Processes

Gaussian Processes (GPs) are a non-parametric Bayesian regression technique in the sense that they do not explicitly define a functional relationship between inputs and outputs (Rasmussen and Williams 2006). Instead, statistical inference is employed to learn dependencies between points in a data set. The joint distribution of the observed target values, $\boldsymbol{y}$, and the function values (the latent variable), $\boldsymbol{f}_*$, at the query points can be written as

$$\begin{bmatrix}\boldsymbol{y}\\ \boldsymbol{f}_*\end{bmatrix} \sim \mathcal{N}(\boldsymbol{0}, \begin{bmatrix}\boldsymbol{K}(\boldsymbol{X},\boldsymbol{X}) + \sigma_n^2\boldsymbol{I}_n & \boldsymbol{K}(\boldsymbol{X},\boldsymbol{X}_*)\\ \boldsymbol{K}(\boldsymbol{X}_*,\boldsymbol{X}) & \boldsymbol{K}(\boldsymbol{X}_*,\boldsymbol{X}_*)\end{bmatrix}) \tag{7}$$

where $\boldsymbol{X}$ is the $d\times n$ design matrix of aggregated input vectors $\boldsymbol{x}$, $\boldsymbol{X}_*$ is a $d\times n_*$ query points matrix, $\boldsymbol{K}(\cdot,\cdot)$ is the GP covariance matrix, $\boldsymbol{I}_n$ is the n-by-n identity matrix, and σ_n^2 is the variance of the observation noise which is assumed to have an independent and identically distributed Gaussian distribution. The predictive conditional distribution for a single query point $f_*|\boldsymbol{X},\boldsymbol{y},\boldsymbol{x}_* \sim \mathcal{N}(\mathbb{E}[f_*],\mathbb{V}[f_*])$ can be derived as

$$\mu = \mathbb{E}[f_*] = \boldsymbol{k}(\boldsymbol{X},\boldsymbol{x}_*)^T[\boldsymbol{K}(\boldsymbol{X},\boldsymbol{X}) + \sigma_n^2\boldsymbol{I}_n]^{-1}\boldsymbol{y} \tag{8}$$

$$\sigma = \mathbb{V}[f_*] = k(\boldsymbol{x}_*,\boldsymbol{x}_*) - \boldsymbol{k}(\boldsymbol{X},\boldsymbol{x}_*)^T[\boldsymbol{K}(\boldsymbol{X},\boldsymbol{X}) + \sigma_n^2\boldsymbol{I}_n]^{-1}\boldsymbol{k}(\boldsymbol{X},\boldsymbol{x}_*) \tag{9}$$

The model selection problem refers to the problem of setting of *hyperparameters* (free parameters in a covariance function) within a family, and comparing across different families. Selection of a covariance function and its parameters is called training of a Gaussian process. These problems and various methods to determine the hyperparameters from training data are discussed in details in Rasmussen and Williams

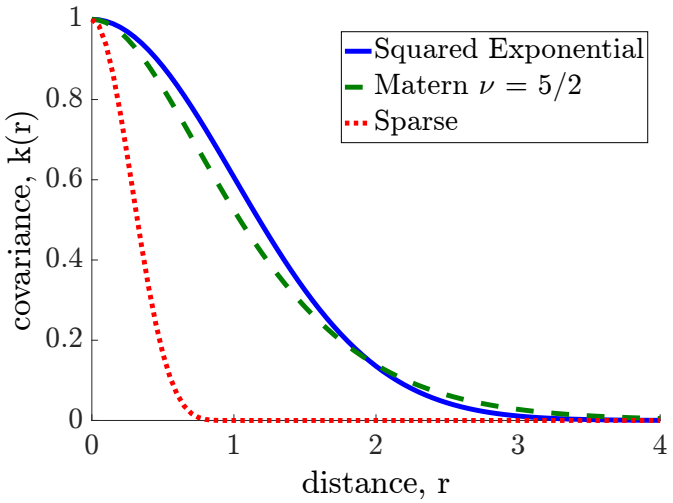

Figure 1: Illustrative examples of the SE, Matérn ($\nu = 5/2$), and Sparse covariance function as the distance parameter is increased from 0 to 4. The length-scale parameter is set to one.

(2006, Chapter 5). The hyperparameters of the covariance and mean function, $\boldsymbol{\theta}$, can be computed by minimization of the negative log of the marginal likelihood (NLML) function.

$$\log p(\boldsymbol{y}|\boldsymbol{X},\boldsymbol{\theta}) = -\frac{1}{2}\boldsymbol{y}^T(\boldsymbol{K}(\boldsymbol{X},\boldsymbol{X}) + \sigma_n^2\boldsymbol{I}_n)^{-1}\boldsymbol{y} - \frac{1}{2}\log|K(\boldsymbol{X},\boldsymbol{X}) + \sigma_n^2\boldsymbol{I}_n| - \frac{n}{2}\log 2\pi \tag{10}$$

3.5.1 Covariance Function

Covariance functions are the main part of any GPs. We define a covariance function using the kernel definition as follows.

Definition 1 (Covariance function)**.** Let $\boldsymbol{x} \in \mathcal{X}$ and $\boldsymbol{x}' \in \mathcal{X}$ be a pair of inputs for a function $k : \mathcal{X} \times \mathcal{X} \to \mathbb{R}$ known as kernel. A kernel is called a covariance function, as the case in Gaussian processes, if it is symmetric, $k(\boldsymbol{x},\boldsymbol{x}') = k(\boldsymbol{x}',\boldsymbol{x})$, and positive semidefinite (PSD):

$$\int k(\boldsymbol{x},\boldsymbol{x}')f(\boldsymbol{x})f(\boldsymbol{x}')d\mu(\boldsymbol{x})d\mu(\boldsymbol{x}') \geq 0 \tag{11}$$

for all $f \in L_2(\mathcal{X},\mu)$.

Given a set of input points $\{\boldsymbol{x}|i = 1 : n\}$, a covariance matrix can be constructed using $\boldsymbol{K}^{[i,j]} = k(\boldsymbol{x}_i,\boldsymbol{x}_j)$ as its entries.

3.5.2 Useful Kernels

The *squared exponential* (SE) covariance function has the form $k(r) = \exp(-\frac{r^2}{2l^2})$ where $r = \|\boldsymbol{x} - \boldsymbol{x}_*\|$ is the distance between two input arguments of the covariance function and l is the *characteristic length-*

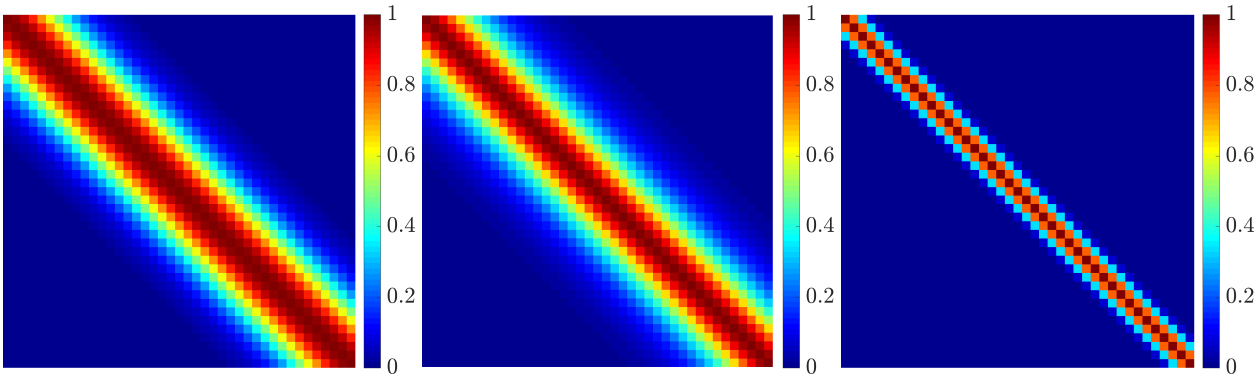

(a) SE (b) Matérn $\nu = 5/2$ (c) Sparse

Figure 2: Corresponding function values from Figure 1 in the kernel space.

scale. This covariance function is the most common kernel used in GPs and is infinitely differentiable. The Matérn family of covariance functions (Stein 1999) has proven powerful features to model structural correlations (Ghaffari Jadidi et al. 2013; Kim and Kim 2013; Ghaffari Jadidi et al. 2014; Kim and Kim 2015). For a single query point $\boldsymbol{x}_*$ the function is given by

$$k(r) = \frac{1}{\Gamma(\nu)2^{\nu-1}}\left[\frac{\sqrt{2\nu}r}{l}\right]^{\nu} K_{\nu}\left(\frac{\sqrt{2\nu}r}{l}\right) \tag{12}$$

where Γ is the Gamma function, $K_{\nu}(\cdot)$ is the modified Bessel function of the second kind of order ν, l is the characteristic length scale, and ν is a positive parameter used to control the smoothness of the covariance. In the limit for $\nu \to \infty$ this covariance function converges to the SE kernel. An intrinsically sparse covariance function is developed in Melkumyan and Ramos (2009). The function is a *stationary* covariance function and its sparseness is controlled through learning the hyperparameters.

Examples of the SE, Matérn ($\nu = 5/2$), and Sparse covariance functions as the distance parameter r increases are shown in Figure 1. The functions are also plotted in kernel space in Figure 2. The diminishing behavior of the Sparse covariance function as the distance parameter exceeds 1 can be seen in the plot which in the corresponding kernel space is represented by mainly non-zero elements on the diagonal part of the covariance matrix.

4 Problem Statement

The problem of robotic information gathering is formulated as a maximization problem subject to finite resources, i.e. a budget b. In Hollinger and Sukhatme (2014), this problem is defined as follows.

Problem 1 (Informative motion planning)**.** Let $\mathcal{A}$ be the space of all possible trajectories and $f_I(\mathcal{P})$ be a function that quantifies the information quality along a trajectory $\mathcal{P}$. Let $f_c(\mathcal{P})$ be a function that returns the cost associated with trajectory $\mathcal{P}$. Given the available budget b, the problem can be formulated as

follows.

$$\mathcal{P}^* = \arg\max_{\mathcal{P}\in\mathcal{A}} f_I(\mathcal{P}) \quad \text{s.t. } f_c(\mathcal{P}) \leq b \tag{13}$$

Now we express the assumptions in RIG algorithms.

Assumption 5. The cost function $f_c(\mathcal{P})$ is strictly positive, monotonically increasing, bounded, and additive such as distance and energy.

Remark 1. The information function $f_I(\mathcal{P})$ can be modular, time-varying modular, or submodular.

The information function assumption follows from Hollinger and Sukhatme (2014), even though we focus our attention on the submodular class of information functions as the information gathered at any future time during navigation depends on prior robot trajectories. Another reason to consider submodular information functions is to avoid information "double-counting". This allows us to develop an information-theoretic convergence criterion for RIG/IIG as the amount of available information remains bounded. The following assumptions are directly from Hollinger and Sukhatme (2014) which in turn are equivalent or adapted from Bry and Roy (2011); Karaman and Frazzoli (2011). The `Steer` function used in Assumption 6 extends nodes towards newly sampled points.

Assumption 6. Let $\boldsymbol{x}_a$, $\boldsymbol{x}_b$, and $\boldsymbol{x}_c$ be three points within radius Δ of each other. Let the trajectory e_1 be generated by $\texttt{Steer}(\boldsymbol{x}_a, \boldsymbol{x}_c, \Delta)$, e_2 be generated by $\texttt{Steer}(\boldsymbol{x}_a, \boldsymbol{x}_b, \Delta)$, and e_3 be generated by $\texttt{Steer}(\boldsymbol{x}_b, \boldsymbol{x}_c, \Delta)$. If $\boldsymbol{x}_b \in e_1$, then the concatenated trajectory $e_2 + e_3$ must be equal to e_1 and have equal cost and information.

This assumption is required as in the limit drawn samples are infinitely close together, and the `Steer` function, cost, and information need to be consistent for any intermediate point.

Assumption 7. There exists a constant $r \in \mathbb{R}_{>0}$ such that for any point $\boldsymbol{x}_a \in \mathcal{X}_f$ there exists an $\boldsymbol{x}_b \in \mathcal{X}_f$, such that 1) the ball of radius r centered at $\boldsymbol{x}_a$ lies inside $\mathcal{X}_f$ and 2) $\boldsymbol{x}_a$ lies inside the ball of radius r centered at $\boldsymbol{x}_b$.

This assumption ensures that there is enough free space near any point for extension of the graph. Violation of this assumption in practice can lead to failure of the algorithm to find a path. We denote the free workspace by $\mathcal{X}_f$.

Assumption 8 (Uniform sampling)**.** [2] Points returned by the sampling function `sample` are independent and identically distributed (i.i.d.) and drawn from a uniform distribution.

[2] Results extend naturally to any absolutely continuous distribution with density bounded away from zero on workspace $\mathcal{X}$ (Karaman and Frazzoli 2011).

4.1 Incremental Informative Motion Planning

Now we define the problem of incremental informative motion planning as follows.

Problem 2 (Incremental informative motion planning)**.** Let $s_{0:t_s} \in \mathcal{S}$ be the current estimate of the state up to time t_s. Let $\mathcal{A}_t$ be the space of all possible trajectories at time t and $f_I(\mathcal{P}_t)$ be a function that quantifies the information quality along a trajectory $\mathcal{P}_t$. Let $f_c(\mathcal{P}_t)$ be a function that returns the cost associated with trajectory $\mathcal{P}_t$. Given the available budget b_t, the problem can be formulated as follows.

$$\mathcal{P}_t^* = \underset{\mathcal{P}_t \in \mathcal{A}_t}{\arg\max}\ f_I(\mathcal{P}_t) \quad \forall\ t > t_s \quad \text{s.t. } f_c(\mathcal{P}_t) \leq b_t \text{ and } S = s_{0:t_s} \tag{14}$$

Remark 2. The state S can include the representation of the environment (map), the robot trajectory, and possibly any other variables defined in the state vector. In general, the information function $f_I(\mathcal{P}_t)$ is responsible for incorporating the state uncertainty in the information gain calculations.

Remark 3. In practice we solve the problem incrementally and use a planning horizon $T > t_s$ that in the limit goes to ∞.

The main difference between Problem 1 and Problem 2 is that in the latter the robot does not have the full knowledge of the environment *a priori*. Therefore Problem 2 is not only the problem of information gathering but also *planning for estimation* as the robot needs to infer the map (and in general its pose in the SLAM [3] problem) sequentially. Note that we do not impose any assumptions on observability of the robot pose and the map, therefore, they can be partially observation as the case in POMDPs.

The aforementioned problems are both in their offline (nonadaptive) and online (adaptive) forms NP-hard (Singh et al. 2009). We build our proposed incremental information gathering algorithm on top of the RIG to solve the interesting problem of autonomous robotic exploration in unknown environments. Furthermore, since the ultimate goal is online applications, we only consider the RIG-tree variant to be extended for sequential planning. This conclusion stems from extensive comparisons of RIG variants provided in Hollinger and Sukhatme (2014). However, we acknowledge that the RIG-graph is an interesting case to consider as under a *partial ordering* assumption it is *asymptotically optimal*.

4.2 RIG Algorithms

The sampling-based RIG algorithms find a trajectory that maximizes an information quality metric with respect to a pre-specified budget constraint (Hollinger and Sukhatme 2014). The RIG is based on RRT*, RRG, and PRM* (Karaman and Frazzoli 2011) and borrow the notion of informative path planning from branch and bound optimization (Binney and Sukhatme 2012). Algorithm 1 shows the RIG-tree algorithm. The functions that are used in the algorithm are explained as follows.

`Cost` – The cost function assigns a strictly positive cost to a collision-free path between two points from the free space $\mathcal{X}_f$.

[3] Simultaneous Localization And Mapping

Algorithm 1 `RIG-tree()`

Require: Step size Δ, budget b, free space $\mathcal{X}_f$, Environment $\mathcal{M}$, start configuration $\boldsymbol{x}_{start}$, near radius r;

// Initialize cost, information, starting node, node list, edge list, and tree
$I_{init} \leftarrow$ `Information`$([\,], \boldsymbol{x}_{start}, \mathcal{M}), C_{init} \leftarrow 0, n \leftarrow \langle \boldsymbol{x}_{start}, C_{init}, I_{init} \rangle$
$\mathcal{V} \leftarrow \{n\}, \mathcal{V}_{closed} \leftarrow \varnothing, \mathcal{E} \leftarrow \varnothing$
while not terminated **do**
    // Sample configuration space of vehicle and find nearest node
    $\boldsymbol{x}_{sample} \leftarrow$ `Sample`$(\mathcal{X}_f)$
    $\boldsymbol{x}_{nearest} \leftarrow$ `Nearest`$(\boldsymbol{x}_{sample}, \mathcal{V} \backslash \mathcal{V}_{closed})$
    $\boldsymbol{x}_{feasible} \leftarrow$ `Steer`$(\boldsymbol{x}_{nearest}, \boldsymbol{x}_{sample}, \Delta)$
    // Find near points to be extended
    $\mathcal{V}_{near} \leftarrow$ `Near`$(\boldsymbol{x}_{feasible}, \mathcal{V} \backslash \mathcal{V}_{closed}, r)$
    for all $n_{near} \in \mathcal{V}_{near}$ **do**
        // Extend towards new point
        $\boldsymbol{x}_{new} \leftarrow$ `Steer`$(\boldsymbol{x}_{near}, \boldsymbol{x}_{feasible}, \Delta)$
        if `NoCollision`$(\boldsymbol{x}_{near}, \boldsymbol{x}_{new}, \mathcal{X}_f)$ **then**
            // Calculate new information and cost
            $I_{new} \leftarrow$ `Information`$(I_{near}, \boldsymbol{x}_{new}, \mathcal{M}), c(\boldsymbol{x}_{new}) \leftarrow$ `Cost`$(\boldsymbol{x}_{near}, \boldsymbol{x}_{new})$
            $C_{new} \leftarrow C_{near} + c(\boldsymbol{x}_{new}), n_{new} \leftarrow \langle \boldsymbol{x}_{new}, C_{new}, I_{new} \rangle$
            if `Prune`(n_{new}) **then**
                delete n_{new}
            else
                // Add edges and nodes
                $\mathcal{E} \leftarrow \cup\{(n_{near}, n_{new})\}, \mathcal{V} \leftarrow \cup\{n_{new}\}$
                // Add to closed list if budget exceeded
                if $C_{new} > b$ **then**
                    $\mathcal{V}_{closed} \leftarrow \mathcal{V}_{closed} \cup \{n_{new}\}$
                end if
            end if
        end if
    end for
end while
return $\mathcal{T} = (\mathcal{V}, \mathcal{E})$

`Information` – This function quantifies the information quality of a collision-free path between two points from the free space $\mathcal{X}_f$.

`Sample` – This function returns i.i.d. samples from $\mathcal{X}_f$.

`Nearest` – Given a graph $\mathcal{G} = (\mathcal{V}, \mathcal{E})$, where $\mathcal{V} \subset \mathcal{X}_f$, and a query point $\boldsymbol{x} \in \mathcal{X}_f$, this function returns a vertex $v \in \mathcal{V}$ that has the "closest" distance to the query point [4].

`Steer` – This function extends nodes towards newly sampled points and allows for constraints on motion of the robot [5].

`Near` – Given a graph $\mathcal{G} = (\mathcal{V}, \mathcal{E})$, where $\mathcal{V} \subset \mathcal{X}_f$, a query point $\boldsymbol{x} \in \mathcal{X}_f$, and a positive real number $r \in \mathbb{R}_{>0}$, this function returns a set of vertices $\mathcal{V}_{near} \subseteq \mathcal{V}$ that are contained in a ball of radius r centered at $\boldsymbol{x}$.

[4] Here we use Euclidean distance.

[5] Through this function, it is possible to make the planner kinodynamic.

`NoCollision` – Given two points $\boldsymbol{x}_a, \boldsymbol{x}_b \in \mathcal{X}_f$, this functions returns **true** if the line segment between $\boldsymbol{x}_a$ and $\boldsymbol{x}_b$ is collision-free and **false** otherwise.

`Prune` – This function implements a pruning strategy to remove nodes that are not "promising". This can be achieved through defining a *partial ordering* for co-located nodes.

In line 2-3 the algorithm initializes the starting node of the graph (tree). In line 6-8, a sample point from workspace $\mathcal{X}$ is drawn and is converted to a feasible point, from its nearest neighbor in the graph. Line 10 extracts all nodes from the graph that are within radius r of the feasible point. These nodes are candidates for extending the graph, and each node is converted to a new node using the `Steer` function in line 13. In line 14-17, if there exists a collision free path between the candidate node and the new node, the information gain and cost of the new node are evaluated. In line 18-25, if the new node does not satisfy a partial ordering condition is pruned, otherwise it is added to the graph. Furthermore, the algorithm checks for the budget constraint violation. The output is a graph that contains a subset of traversable paths with maximum information gain.

4.3 System Dynamics

The equation of motion of the robot is governed by the nonlinear partially observable equation as follows.

$$\boldsymbol{x}_{t+1}^{-} = f(\boldsymbol{x}_t, \boldsymbol{u}_t, \boldsymbol{w}_t) \quad \boldsymbol{w}_t \sim \mathcal{N}(\boldsymbol{0}, \boldsymbol{Q}_t) \tag{15}$$

moreover, with appropriate linearization at the current state estimate, we can predict the state covariance matrix as

$$\Sigma_{t+1}^{-} = \boldsymbol{F}_t \Sigma_t \boldsymbol{F}_t^T + \boldsymbol{W}_t \boldsymbol{Q}_t \boldsymbol{W}_t^T \tag{16}$$

where $\boldsymbol{F}_t = \frac{\partial f}{\partial \boldsymbol{x}}|_{\boldsymbol{x}_t, \boldsymbol{u}_t}$ and $\boldsymbol{W}_t = \frac{\partial f}{\partial \boldsymbol{w}}|_{\boldsymbol{x}_t, \boldsymbol{u}_t}$ are the Jacobian matrices calculated with respect to $\boldsymbol{x}$ and $\boldsymbol{w}$, respectively.

5 IIG: Incrementally-exploring Information Gathering

In this section, we present the IIG algorithm which is essentially RIG with an information-theoretic convergence condition. The algorithmic implementation of IIG is shown in Algorithm 2. We employ IIG to solve the robotic exploration problem with the partially observable state. Both RIG and IIG, through incremental sampling, search the space of possible trajectories to find the maximally informative path; however, due to the automatic convergence of the IIG, it is possible to run the algorithm online without the full knowledge of the state, i.e. the map and robot poses.

We introduce the relative information contribution (RIC) criterion to detect the convergence of the search. The motivation behind this definition is that the number of nodes constantly increases unless an aggressive pruning strategy is used. However, an aggressive pruning strategy leads to potentially

Algorithm 2 `IIG-tree()`

Require: Step size Δ, budget b, free space $\mathcal{X}_f$, Environment $\mathcal{M}$, start configuration $\boldsymbol{x}_{start}$, near radius r, relative information contribution threshold δ_{RIC}, averaging window size n_{RIC};

// Initialize cost, information, starting node, node list, edge list, and tree
$I_{init} \leftarrow$ `Information`$([\,], \boldsymbol{x}_{start}, \mathcal{M}), C_{init} \leftarrow 0, n \leftarrow \langle \boldsymbol{x}_{start}, C_{init}, I_{init} \rangle$
$\mathcal{V} \leftarrow \{n\}, \mathcal{V}_{closed} \leftarrow \varnothing, \mathcal{E} \leftarrow \varnothing$
$n_{sample} \leftarrow 0$ // Number of samples
$I_{RIC} \leftarrow \varnothing$ // Relative information contribution
while `AverageRIC`$(I_{RIC}, n_{RIC}) > \delta_{RIC}$ **do**
    // Sample configuration space of vehicle and find nearest node
    $\boldsymbol{x}_{sample} \leftarrow$ `Sample`$(\mathcal{X}_f)$
    $n_{sample} \leftarrow n_{sample} + 1$
    $\boldsymbol{x}_{nearest} \leftarrow$ `Nearest`$(\boldsymbol{x}_{sample}, \mathcal{V} \backslash \mathcal{V}_{closed})$
    $\boldsymbol{x}_{feasible} \leftarrow$ `Steer`$(\boldsymbol{x}_{nearest}, \boldsymbol{x}_{sample}, \Delta)$
    // Find near points to be extended
    $\mathcal{V}_{near} \leftarrow$ `Near`$(\boldsymbol{x}_{feasible}, \mathcal{V} \backslash \mathcal{V}_{closed}, r)$
    for all $n_{near} \in \mathcal{V}_{near}$ **do**
        // Extend towards new point
        $\boldsymbol{x}_{new} \leftarrow$ `Steer`$(\boldsymbol{x}_{near}, \boldsymbol{x}_{feasible}, \Delta)$
        if `NoCollision`$(\boldsymbol{x}_{near}, \boldsymbol{x}_{new}, \mathcal{X}_f)$ **then**
            // Calculate new information and cost
            $I_{new} \leftarrow$ `Information`$(I_{near}, \boldsymbol{x}_{new}, \mathcal{M}), c(\boldsymbol{x}_{new}) \leftarrow$ `Cost`$(\boldsymbol{x}_{near}, \boldsymbol{x}_{new})$
            $C_{new} \leftarrow C_{near} + c(\boldsymbol{x}_{new}), n_{new} \leftarrow \langle \boldsymbol{x}_{new}, C_{new}, I_{new} \rangle$
            if `Prune`(n_{new}) **then**
                delete n_{new}
            else
                $I_{RIC} \leftarrow$ `append`$(I_{RIC}, (\frac{I_{new}}{I_{near}} - 1)/n_{sample})$ // Equation (18)
                $n_{sample} \leftarrow 0$ // Reset sample counter
                // Add edges and nodes
                $\mathcal{E} \leftarrow \cup\{(n_{near}, n_{new})\}, \mathcal{V} \leftarrow \cup\{n_{new}\}$
                // Add to closed list if budget exceeded
                if $C_{new} > b$ **then**
                    $\mathcal{V}_{closed} \leftarrow \mathcal{V}_{closed} \cup \{n_{new}\}$
                end if
            end if
        end if
    end for
end while
return $\mathcal{T} = (\mathcal{V}, \mathcal{E})$

pruning nodes that can be part of optimal solutions [6]. Even though the algorithm continues to add nodes, it is possible to evaluate the contribution of each added node in the relative information sense. In other words, adding nodes does not affect the convergence of the algorithm, but the amount of information the algorithm can collect by continuing the search. We define the RIC of a node as follows.

Definition 2 (Relative Information Contribution)**.** In Algorithm 2, let $\boldsymbol{x}_{new} \in \mathcal{X}_f$ be a reachable point

[6] Note that more than one optimal trajectory at each time can exist, e.g. when the robot needs to explore two equally important directions.

through a neighboring node $n_{near} \in \mathcal{V}$ returned by the function `Near`(). Let I_{new} and I_{near} be the information values of their corresponding nodes returned by the function `Information`(). The relative information contribution of node n_{new} is defined as

$$RIC \triangleq \frac{I_{new}}{I_{near}} - 1 \tag{17}$$

Equation (17) is conceptually important as it defines the amount of information gain relative to a neighboring point in the IIG graph. In practice, the number of samples it takes before the algorithm finds a new node becomes important. Thus we define penalized relative information contribution that is computed in line 24.

Definition 3 (Penalized Relative Information Contribution)**.** Let RIC be the relative information contribution computed using Equation (17). Let n_{sample} be the number of samples it takes to find the node n_{new}. The penalized relative information contribution is defined as

$$I_{RIC} \triangleq \frac{RIC}{n_{sample}} \tag{18}$$

An appealing property of I_{RIC} is that it is non-dimensional, and it does not depend on the actual calculation/approximation of the information values. In practice, as long as the information function satisfies the RIG/IIG requirements, using the following condition, IIG algorithm converges. Let δ_{RIC} be a threshold that is used to detect the convergence of the algorithm. Through averaging I_{RIC} values over a window of size n_{RIC}, we ensure that continuing the search will not add any significant amount of information to the IIG graph. In Algorithm 2, this condition is shown in line 6 by function `AverageRIC`.

Remark 4. In Algorithm 2, δ_{RIC} sets the planning horizon from the information gathering point of view. Through using smaller values of δ_{RIC} the planner can reach further points in both spatial and belief space. In other words, if $\delta_{RIC} \to 0$, then $T \to \infty$.

6 Information Functions Algorithms

We propose two algorithms together with their variations to approximate the information gain at any sampled point from the free workspace. The information function in RIG/IIG algorithms often causes a bottleneck and computationally dominates the other parts. Therefore, even for offline calculations, it is important to have access to functions that, concurrently, are computationally tractable and can capture the essence of information gathering. We emphasize that the information functions are directly related to the employed sensors. However, once the model is provided and incorporated into the estimation/prediction algorithms, the information-theoretic aspects of the provided algorithms remain the same.

The information functions that are proposed are different in nature. First, we discuss MI-based information functions whose calculations explicitly depend on the sensor model. We provide two variants

of the MI Algorithm in Ghaffari Jadidi et al. (2015, 2016) that are based on forward and inverse sensor model map predictions. We also present an algorithm to approximate MI upper bound which reveals the maximum achievable information gain.

Then, we exploit the property of GPs to approximate the information gain. In Equation (9), the variance calculation does not depend on the target vector (measurements). In this case, the information gain can be calculated using map prior and posterior variances which removes the need for relying on a specific sensor model and calculating the expectation over future measurements. Once we established GP Variance Reduction (GPVR) algorithm, we then use the expected kernel notion to propagate pose uncertainty into the covariance function resulting in Uncertain GP Variance Reduction (UGPVR) algorithm. In particular, these two information functions are interesting for the following reasons:

(i) Unlike MI-based (direct information gain calculation), they are non-parametric.

(ii) GPVR-based information functions provide a systematic way to incorporate pose uncertainty into information gathering frameworks.

(iii) In the case of incomplete knowledge about the quantity of interest in an unknown environment, they allow for *active learning* [7].

6.1 Mutual Information

To be able to calculate MI using map prediction we need to update the map after every measurement prediction. It is possible to perform map prediction using a forward or inverse sensor model. Typically using an inverse sensor model results in simpler calculations. Nevertheless, we provide two algorithms that use both types of map predictions. First, we define necessary parameters required in the proposed algorithms.

Definition 4 (Map saturation probability)**.** The probability that the robot is completely confident about the occupancy status of a point is defined as p_{sat}.

Definition 5 (Map saturation entropy)**.** The entropy of a point from a map whose occupancy probability is p_{sat}, is defined as $h_{sat} \triangleq H(p_{sat})$.

The defined parameters are relevant since they prevent the exhaustive search for information in "less important" areas. The MI-based information function using a forward sensor model implementation is shown in Algorithm 3. In line 4, the predicted measurement for beam k is computed using ray casting in the current map estimate. In line 7, for each beam k, the algorithm adds the total map entropy along beam k to the information gain, I. In line 11-14, the algorithm skips any map point whose entropy surpasses the saturation entropy and deducts its entropy from I. In line 15-28, the map conditional entropy by

[7] Although this is one of the most interesting aspects of GPVR-based information functions, it is beyond the scope of this article, and we leave it as a possible extension of this work.

Algorithm 3 `InformationMI()`

Require: Robot pose or desired location, current map estimate m, sensor model, saturation entropy h_{sat};

1: $\bar{m} \leftarrow m$
2: $I \leftarrow 0$
3: **for** all k **do**
4: Compute $\hat{z}_{t+1}^{[k]}$ and $\mathcal{I}_{t+1}^{[k]}$ using ray casting in m
5: // Current map entropy along beam k
6: $h = -\sum_{i \in \mathcal{I}_{t+1}^{[k]}} [\bar{m}^{[i]} \log(\bar{m}^{[i]}) + (1 - \bar{m}^{[i]}) \log(1 - \bar{m}^{[i]})]$
7: $I = I + h$
8: // Calculate map conditional entropy along beam k
9: **for** $i \in \mathcal{I}_{t+1}^{[k]}$ **do**
10: $h_i = -[\bar{m}^{[i]} \log(\bar{m}^{[i]}) + (1 - \bar{m}^{[i]}) \log(1 - \bar{m}^{[i]})]$
11: **if** $h_i < h_{sat}$ **then**
12: $I = I - h_i$
13: **continue**
14: **end if**
15: $\bar{h} \leftarrow 0$
16: **for** all $z \leq \hat{z}_{t+1}^{[k]}$ **do**
17: // Calculate marginal measurement probability p_z
18: $p_1 \leftarrow p(\hat{z}_{t+1}^{[k]} | M = 0)$
19: $p_2 \leftarrow 0$
20: **for** $j \in \mathcal{I}_{t+1}^{[k]}$ **do**
21: $p_1 \leftarrow p_1 (1 - m^{[j]})$
22: $p_2 \leftarrow p_2 + p(\hat{z}_{t+1}^{[k]} | M = m^{[j]}) m^{[j]} \prod_{l<j} (1 - m^{[l]})$
23: **end for**
24: $p_z \leftarrow p_1 + p_2$
25: // Map prediction at point i along beam k
26: $\bar{m}^{[i]} \leftarrow p_z^{-1} p(\hat{z}_{t+1}^{[k]} | M = m^{[i]}) m^{[i]} \prod_{l<i} (1 - m^{[l]})$
27: $\bar{h} \leftarrow \bar{h} + p_z [\bar{m}^{[i]} \log(\bar{m}^{[i]}) + (1 - \bar{m}^{[i]}) \log(1 - \bar{m}^{[i]})]$
28: **end for**
29: $I \leftarrow I + \bar{h} s_z^{-1}$
30: **end for**
31: **end for**
32: **return** I (total information gain), $\bar{m}$ (estimated map)

integrating over future measurement is calculated and in line 29 it is subtracted from initial map entropy using an appropriate numerical integration resolution, s_z^{-1}.

In practice, the map prediction using a forward sensor model used in Algorithm 3 for multi-step predictions may lead to poor map quality and, consequently, inaccurate information gain. Therefore, we develop Algorithm 4 that employs an inverse sensor model technique for map prediction. Algorithm 4 performs well in practice for multi-step predictions. The main difference can be seen in line 26-30 where map prediction is performed using free point belief, b_{free}, and occupied point belief, b_{occ}. The predicted probabilities are clamped using $\epsilon > 0$ which is a small number relative to p_{sat} to avoid losing numerical

Algorithm 4 `InformationMI2()`

Require: Robot pose or desired location, current map estimate m, sensor model, saturation probability p_{sat}, saturation entropy h_{sat}, free point belief b_{free}, occupied point belief b_{occ};

$\bar{m} \leftarrow m$
$I \leftarrow 0$
for all k **do**
  Compute $\hat{z}_{t+1}^{[k]}$ and $\mathcal{I}_{t+1}^{[k]}$ using ray casting in m
  // Current map entropy along beam k
  $h = -\sum_{i \in \mathcal{I}_{t+1}^{[k]}} [\bar{m}^{[i]} \log(\bar{m}^{[i]}) + (1 - \bar{m}^{[i]}) \log(1 - \bar{m}^{[i]})]$
  $I = I + h$
  // Calculate map conditional entropy along beam k
  for $i \in \mathcal{I}_{t+1}^{[k]}$ **do**
    $h_i = -[\bar{m}^{[i]} \log(\bar{m}^{[i]}) + (1 - \bar{m}^{[i]}) \log(1 - \bar{m}^{[i]})]$
    if $h_i < h_{sat}$ **then**
      $I = I - h_i$
      continue
    end if
    $\bar{h} \leftarrow 0$
    for all $z \leq \hat{z}_{t+1}^{[k]}$ **do**
      // Calculate marginal measurement probability p_z
      $p_1 \leftarrow p(\hat{z}_{t+1}^{[k]} | M = 0)$
      $p_2 \leftarrow 0$
      for $j \in \mathcal{I}_{t+1}^{[k]}$ **do**
        $p_1 \leftarrow p_1 (1 - m^{[j]})$
        $p_2 \leftarrow p_2 + p(\hat{z}_{t+1}^{[k]} | M = m^{[j]}) m^{[j]} \prod_{l<j} (1 - m^{[l]})$
      end for
      $p_z \leftarrow p_1 + p_2$
      // Map prediction at point i along beam k using inverse sensor model
      if `isFree`$(\bar{m}^{[i]})$ **then**
        $\bar{m}^{[i]} = \max(p_{sat} - \epsilon, b_{free} * \bar{m}^{[i]})$
      else
        $\bar{m}^{[i]} = \min(1 - p_{sat} + \epsilon, b_{occ} * \bar{m}^{[i]})$
      end if
      $\bar{h} \leftarrow \bar{h} + p_z [\bar{m}^{[i]} \log(\bar{m}^{[i]}) + (1 - \bar{m}^{[i]}) \log(1 - \bar{m}^{[i]})]$
    end for
    $I \leftarrow I + \bar{h} s_z^{-1}$
  end for
end for
return I (total information gain), $\bar{m}$ (estimated map)

computation accuracy.

It is also interesting to calculate an upper bound for the information gain. Given the provided algorithms, it is trivial to calculate MI upper bound using the total amount of map entropy in the current perception field of the robot. It is faster to compute the upper bound as it only shows the uncertainty from the current map and it does not consider any gain from future measurements. However, in practice, it can be useful for fast and online predictions. More details regarding the difference between maximizing

Algorithm 5 `InformationMIUB()`

Require: Robot pose or desired location, current map estimate m, sensor model, saturation entropy h_{sat};

$\bar{m} \leftarrow m$
$I_{UB} \leftarrow 0$
for all k **do**
    Compute $\hat{z}_{t+1}^{[k]}$ and $\mathcal{I}_{t+1}^{[k]}$ using ray casting in m
    // Current map entropy along beam k
    $h = -\sum_{i \in \mathcal{I}_{t+1}^{[k]}} [\bar{m}^{[i]} \log(\bar{m}^{[i]}) + (1 - \bar{m}^{[i]}) \log(1 - \bar{m}^{[i]})]$
    $I_{UB} = I_{UB} + h$
    // Check for saturated points along beam k
    for $i \in \mathcal{I}_{t+1}^{[k]}$ **do**
        $h_i = -[\bar{m}^{[i]} \log(\bar{m}^{[i]}) + (1 - \bar{m}^{[i]}) \log(1 - \bar{m}^{[i]})]$
        if $h_i < h_{sat}$ **then**
            $I_{UB} = I_{UB} - h_i$
            continue
        end if
        Update the map points $\bar{m}^{[i]}$ along beam k using forward or inverse sensor model
    end for
end for
return I_{UB} (total information gain), $\bar{m}$ (estimated map)

mutual information and entropy are discussed in Guestrin et al. (2005); Krause et al. (2008).

Lemma 3 (Information gain upper bound)**.** *For any location in the map, the information gain upper bound is given by the total map entropy calculated using map points in the perception field of the robot at the same location.*

Proof. From Lemma 2 and Theorem 4; $0 \leq I(M;Z) = H(M) - H(M|Z) \leq H(M)$ which extends to any sub-map $\mathcal{M}_{sub}$ that is in the perception field of the robot. Note that MI beyond the perception field is zero as $\forall\, M \in \mathcal{M} \setminus \mathcal{M}_{sub}, M \perp Z$. □

Algorithm 5 shows the MI Upper Bound (MIUB) information function in which the integration over predicted measurement is omitted. However, to avoid information double-counting, it is still required to update the map estimate after each function call. Furthermore, the MIUB calculation can be integrated into Algorithm 3 and 4 with an insignificant computational load.

6.2 GP Variance Reduction

Variance reduction is the essence of information gathering. Since predictive variance calculation in Equation (9), does not depend on observations, we can come up with a non-parametric algorithm to estimate variance reduction throughout dense belief representation of the map. For the problem of informative path planning, a similar approach is used in Binney et al. (2013) where the reduction in the trace of the covariance function is considered as the objective function (A-optimality). Here, we are interested in approximating the mutual information through entropy reduction, i.e. using determinant of the covariance

matrix (D-optimality) (Pukelsheim 2006). This is mainly to keep the proposed IIG framework agnostic about the choice of information functions. We treat each map point as a continuous random variable that is normally distributed. Therefore we use differential entropy formulation for mutual information approximation.

Lemma 4 (Differential entropy of a Gaussian random variable)**.** *Let $X \sim \mathcal{N}(\mu, \sigma^2)$. The differential entropy of X can be derived as follows.*

$$h(X) = \frac{1}{2}\log(2\pi e\sigma^2) \tag{19}$$

Proof. The proof follows from the definition of differential entropy and direct integration (Cover and Thomas 1991). □

Proposition 9. *Let $X_1, X_2, ..., X_n$ have a multivariate normal distribution with covariance matrix $\boldsymbol{K}$. The mutual information between X and observations Z can be approximated as*

$$\hat{I}(X;Z) = \sum_{i=1}^{n} \log(\sigma_{X_i}) - \sum_{i=1}^{n} \log(\sigma_{X_i|Z}) \tag{20}$$

where σ_{X_i} and $\sigma_{X_i|Z}$ are marginal variances for X_i before and after incorporating observations Z, i.e. prior and posterior marginal variances.

Proof. Using marginalization property of normal distribution, Lemma 1, for every X_i we have $\mathbb{V}[X_i] = \boldsymbol{K}^{[i,i]}$. From Lemma 4, the mutual information for X_i can be written as

$$\hat{I}^{[i]}(X_i;Z) = \log(\sigma_{X_i}) - \log(\sigma_{X_i|Z}) \tag{21}$$

and the total mutual information can be calculated as $\hat{I}(X;Z) = \sum_{i=1}^{n} \hat{I}^{[i]}(X_i;Z)$. □

Algorithm 6 shows the details of GPVR information function [8]. Based on the training points generated from predicted measurement $\boldsymbol{z}$, a sub-map from the current map estimate using nearest neighbor search is found, line 3-8. In line 9-13, GP predictive variances are computed using covariance function k with the same hyperparameters learned for the map inference. In line 14-17, using Bayesian Committee Machine (BCM) fusion (Tresp 2000) the predictive marginal posterior variance is calculated and the information gain is updated consequently. The Cholesky factorization is the most computationally expensive operation of the algorithm. However, it is possible to exploit a sparse covariance matrix such as the kernel in Melkumyan and Ramos (2009) or use a cut-off distance for the covariance function [9] to speed up the algorithm.

[8] The algorithm uses MATLAB-style operations for matrix inversion, Cholesky factorization, and dot product with matrix inputs.

[9] The semi-positive definiteness of the covariance matrix needs to be preserved.

Algorithm 6 `InformationGPVR()`

Require: Robot pose or desired location $\boldsymbol{p}$, current map estimate m, covariance function k, sensor noise σ_n^2;

$\bar{\sigma} \leftarrow \sigma$ // global map variance
$I \leftarrow 0$
for all k **do**
    Compute $\hat{z}_{t+1}^{[k]}$ and $\mathcal{I}_{t+1}^{[k]}$ using ray casting in m
end for
$\mathcal{D} \leftarrow \texttt{TrainingData}(\boldsymbol{p}, \boldsymbol{z})$
// Find the global sub-map using nearest neighbor search
$\mathcal{M}_{\mathcal{D}} \leftarrow \texttt{Near}(\mathcal{D})$
$\boldsymbol{K} \leftarrow k(\boldsymbol{X}, \boldsymbol{X}), \boldsymbol{K}_* \leftarrow k(\boldsymbol{X}, \boldsymbol{X}_*)$ // $\boldsymbol{X} \in \mathcal{M}_{\mathcal{D}}$ and $\boldsymbol{X}_* \in \mathcal{D}$
// Calculate vector of diagonal variances for training/test points
$\boldsymbol{k}_{**} \leftarrow k(\boldsymbol{X}_*, \boldsymbol{X}_*, \text{'diag'})$
$\boldsymbol{L} \leftarrow \texttt{Cholesky}(\boldsymbol{K} + \sigma_n^2 \boldsymbol{I})$, $\boldsymbol{V} \leftarrow \boldsymbol{L} \backslash \boldsymbol{K}_*$
$\boldsymbol{v} \leftarrow \boldsymbol{k}_{**} - \texttt{dot}(\boldsymbol{V}, \boldsymbol{V})^T$ // dot product
for all $i \in \mathcal{M}_{\mathcal{D}}$ **do**
    $\bar{\sigma}^{[i]} \leftarrow ((\sigma^{[i]})^{-1} + (\boldsymbol{v}^{[i]})^{-1})^{-1}$ // BCM fusion
    $I \leftarrow I + \log(\sigma^{[i]}) - \log(\bar{\sigma}^{[i]})$
end for
return I (total information gain), $\bar{\sigma}$ (estimated map variance)

6.3 Uncertain GP Variance Reduction

Thus far, the developed information functions do not incorporate uncertainties of other state variables that are jointly distributed with the map (such as the robot pose) in information gain calculation. We define the modified kernel $\tilde{k}$ as follows.

Definition 6 (Modified kernel)**.** Let $k(x, x_*)$ be a kernel and $X \in \mathcal{X}$ a random variable that is distributed according to a probability distribution function $p(x)$. The modified kernel is defined as its expectation with respect to $p(x)$, therefore we can write

$$\tilde{k} = \mathbb{E}[k] = \int_{\mathcal{X}} k p(x) dx \tag{22}$$

Through replacing the kernel function in Algorithm 6 with the modified kernel we can propagate the robot pose uncertainty in the information gain calculation. Intuitively, under the presence of uncertainty in other state variables that are correlated with the map, the robot does not take greedy actions as the amount of available information calculated using the modified kernel is less than the original case. Therefore, the chosen actions are relatively more conservative. The integration in Equation 22 can be numerically approximated using Monte-Carlo or Gauss-Hermite quadrature techniques (Davis and Rabinowitz 1984; Press et al. 1996). In the case of a Gaussian assumption for the robot pose, Gauss-Hermite quadrature provides a better accuracy and efficiency trade-off and is preferred.

Algorithm 7 shows UGPVR information function. The difference with GPVR is that the input location is not deterministic, i.e. it is approximated as a normal distribution $\mathcal{N}(\boldsymbol{p}, \Sigma)$, and the covariance function is

Algorithm 7 `InformationUGPVR()`

Require: Robot pose or desired location $\boldsymbol{p}$ with covariance Σ, current map estimate m, modified covariance function $\tilde{k}$, sensor noise σ_n^2;

1: $\bar{\sigma} \leftarrow \sigma$ // global map variance
2: $I \leftarrow 0$
3: **for** all k **do**
4: Compute $\hat{z}_{t+1}^{[k]}$ and $\mathcal{I}_{t+1}^{[k]}$ using ray casting in m
5: **end for**
6: $\mathcal{D} \leftarrow$ `TrainingData`$(\boldsymbol{p}, \boldsymbol{z})$
7: // Find the global sub-map using nearest neighbor search
8: $\mathcal{M}_{\mathcal{D}} \leftarrow$ `Near`$(\mathcal{D})$
9: $\boldsymbol{K} \leftarrow \tilde{k}(\boldsymbol{X}, \boldsymbol{X}, \Sigma), \boldsymbol{K}_* \leftarrow \tilde{k}(\boldsymbol{X}, \boldsymbol{X}_*, \Sigma)$ // $\boldsymbol{X} \in \mathcal{M}_{\mathcal{D}}$ and $\boldsymbol{X}_* \in \mathcal{D}$
10: // Calculate vector of diagonal variances for training/test points
11: $\boldsymbol{k}_{**} \leftarrow \tilde{k}(\boldsymbol{X}_*, \boldsymbol{X}_*, \Sigma,$'diag')
12: $\boldsymbol{L} \leftarrow$ `Cholesky`$(\boldsymbol{K} + \sigma_n^2 \boldsymbol{I})$, $\boldsymbol{V} \leftarrow \boldsymbol{L} \backslash \boldsymbol{K}_*$
13: $\boldsymbol{v} \leftarrow \boldsymbol{k}_{**} -$ `dot`$(\boldsymbol{V}, \boldsymbol{V})^T$ // dot product
14: **for** all $i \in \mathcal{M}_{\mathcal{D}}$ **do**
15: $\bar{\sigma}^{[i]} \leftarrow ((\sigma^{[i]})^{-1} + (v^{[i]})^{-1})^{-1}$ // BCM fusion
16: $I \leftarrow I + \log(\sigma^{[i]}) - \log(\bar{\sigma}^{[i]})$
17: **end for**
18: **return** I (total information gain), $\bar{\sigma}$ (estimated map variance)

replaced by its modified version. Given the initial pose belief, the pose uncertainty propagation on the IIG graph can be performed using the robot motion model, i.e. using Equations (15) and (16). Since we already calculate the information gain for each node, it suffices to consider the worst-case covariance prediction. This approach is computationally more efficient and does not rely on any specific SLAM *front-end* for loop-closure detection.

7 Path Extraction and Selection

The RIG/IIG-tree algorithm provides a tree (graph) that is already expanded in the state space using maximum information gathering policy. However, we need to extract the maximally informative path as the selected action. For robotic exploration scenarios, it is not possible to traverse all the available trajectories because after execution of one trajectory the state belief is updated and previous predictions are obsolete [10]. Therefore, one possible solution will be finding a path in the IIG tree that maximizes the information gain.

We provide a heuristic algorithm based on a voting method. Algorithm 8 shows the implementation of the proposed method. The algorithm first finds all possible paths using a preorder *depth first search*, function `DFSpreorder`, and then removes paths that are shorter than a minimum length (using parameter $0 < \kappa < 1$), line 2-10. Then each path is compared with others using the following strategy. If two paths have more than a specified number nodes in common, then we penalize the shorter path by a negative

[10] Here we assume the robot remains committed to the selected action.

Algorithm 8 `PathSelection()`

Require: RIG/IIG tree $\mathcal{T}$, maximum path length l_{max}, maximum similar nodes n_{sim};

1: // Find all leaves using depth first search
2: $\mathcal{V}_{leaves} = \texttt{DFSpreorder}(\mathcal{T})$
3: // Find all paths by starting from each leaf and following parent nodes
4: $\mathcal{P}_{all} = \texttt{Paths2root}(\mathcal{T}, \mathcal{V}_{leaves})$
5: $l_{min} = \texttt{ceil}(\kappa l_{max})$ // Minimum path length, $0 < \kappa < 1$
6: **for** all $\mathcal{P} \in \mathcal{P}_{all}$ **do**
7: **if** $\texttt{length}(\mathcal{P}) \leq l_{min}$ **then**
8: **Delete** $\mathcal{P}$
9: **end if**
10: **end for**
11: $l = \texttt{length}(\mathcal{P}_{all})$
12: $vote = \texttt{zeros}(l, 1)$
13: // Find longest independent paths
14: **for** all $i < l - 1$ **do**
15: **for** all $i + 1 < j < l$ **do**
16: $l_{min} = \min(\texttt{length}(\mathcal{P}_i), \texttt{length}(\mathcal{P}_j))$
17: // Find number of common nodes between path i and j
18: $n_{com} = \texttt{SimilarNodes}(\mathcal{P}_i, \mathcal{P}_j)$
19: **if** $n_{com}/l_{min} > n_{sim}$ **then**
20: **if** $\texttt{length}(\mathcal{P}_i) > \texttt{length}(\mathcal{P}_j)$ **then**
21: $vote^{[i]} = vote^{[i]} + 1$
22: $vote^{[j]} = vote^{[j]} - 1$
23: **else**
24: $vote^{[i]} = vote^{[i]} - 1$
25: $vote^{[j]} = vote^{[j]} + 1$
26: **end if**
27: **else** // Two independent paths
28: $vote^{[i]} = vote^{[i]} + 1$
29: $vote^{[j]} = vote^{[j]} + 1$
30: **end if**
31: **end for**
32: **end for**
33: // Find paths with maximum vote and select the maximally informative path
34: $\mathcal{P}_{max} = \texttt{MaxVotePath}(\mathcal{P}_{all}, vote)$
35: $\mathcal{P}_I = \texttt{MaxInformativePath}(\mathcal{P}_{max})$
36: **return** $\mathcal{P}_I$

vote and encourage the longer path by a positive vote. However, if two paths do not have many common nodes, then they are considered as two independent paths, and they receive positive votes, line 11-32. The function `SimilarNodes` returns the number of overlapping nodes between two paths. In line 34, the function `MaxVotePath` returns all paths that have the maximum number of votes. There is usually more than one path with the maximum vote, therefore, in line 35, the function `MaxInformativePath` selects the path that overall has the maximum information gain.

8 Information-theoretic Robotic Exploration

In this section, we present the information-theoretic basis for applying the IIG-tree algorithm to solve the autonomous robotic exploration problem. Since the developed algorithm does not rely on geometric features (frontiers) for map exploration, an alternative criterion is required for mission termination. We use the entropy independence bound theorem to leverage such a criterion.

Theorem 10 (Independence bound on entropy)**.** *Let $X_1, X_2, ..., X_n$ be drawn according to $p(x_1, x_2, ..., x_n)$. Then*

$$H(X_1, X_2, ..., X_n) \leq \sum_{i=1}^{n} H(X_i) \tag{23}$$

with equality if and only if the X_i are Independent.

Proof. The proof follows directly from Theorem 1 and 4. □

This theorem states that the joint entropy is always smaller than sum of entropies independently and both sides are equal if and only if the random variables are independent. We start from this inequality and prove that for robotic information gathering or map exploration the least upper bound of the average map entropy that is calculated by assuming independence between map points can be a threshold for mission termination. This is formally stated in the following theorem.

Theorem 11 (The least upper bound of the average map entropy)**.** *Let $n \in \mathbb{N}$ be the number of map points. In the limit, for a completely explored occupancy map, the least upper bound of the average map entropy is given by $H(p_{sat})$.*

Proof. From Theorem 10 and through multiplying each side of the inequality by $\frac{1}{n}$, we can write the average map entropy as

$$\frac{1}{n} H(M) < \frac{1}{n} \sum_{i=1}^{n} H(M = m^{[i]}) \tag{24}$$

by taking the limit as $p(m) \to p_{sat}$, then

$$\lim_{p(m) \to p_{sat}} \frac{1}{n} H(M) < \lim_{p(m) \to p_{sat}} \frac{1}{n} \sum_{i=1}^{n} H(M = m^{[i]})$$

$$\lim_{p(m) \to p_{sat}} \frac{1}{n} H(M) < H(p_{sat})$$

$$\sup \frac{1}{n} H(M) = H(p_{sat}) \tag{25}$$

□

The result from Theorem 11 is useful because the calculation of the right hand side of the inequality (24) is trivial. In contrast, calculation of the left hand side assuming the map belief is represented

by a multi-variate Gaussian, requires maintaining the full map covariance matrix and computation of its determinant. This is not practical, since the map often has a dense belief representation and can be theoretically expanded unbounded (to a very large extent). In the following, we preset some notable remarks and consequences of Theorem 11.

Remark 5. The result from Theorem 11 also extends to continuous random variables and differential entropy.

Remark 6. Note that we do not assume any distribution for map points. The entropy can be calculated either with the assumption that the map points are normally distributed or treating them as Bernoulli random variables.

Remark 7. Since $0 < p_{sat} < 1$ and $H(p_{sat}) = H(1 - p_{sat})$, one saturation entropy can be set for the entire map.

Corollary 12 (information gathering termination)**.** *Given a saturation entropy h_{sat}, the problem of search for information gathering for desired random variables $X_1, X_2, ..., X_n$ whose support is alphabet $\mathcal{X}$, can be terminated when $\frac{1}{n}\sum_{i=1}^{n} H(X_i) \leq h_{sat}$.*

Corollary 13 (Map exploration termination)**.** *The problem of autonomous robotic exploration for mapping can be terminated when $\frac{1}{n}\sum_{i=1}^{n} H(M = m^{[i]}) \leq H(p_{sat})$.*

The Corollary 12 generalizes the notion of exploration in the sense of information gathering. Therefore, regardless of the quantity of interest, we can provide a stopping criterion for the exploration mission. The Corollary 13 is of great importance for the classic robotic exploration for map completion problem as there is no need to resort to geometric frontiers with a specific cluster size to detect map completion. Another advantage of setting a threshold in the information space is the natural consideration of uncertainty in the estimation process before issuing a mission termination signal.

9 Results and Discussion

In this section, we examine the proposed algorithms in several scenarios. We first design experiments for comparison of information functions under various sensor parameters such as the number of beams and the sensor range, and their effects on the convergence of IIG. Although the primary objective of this experiment is to evaluate the performance of IIG using each information function, it can also be seen as a sensor selection problem. In other words, given the map of an environment and a number of sensors with different characteristics, we wish to select the sensor that has a reasonable balance of performance and cost. However, we do not emphasize this aspect as the main objective of the test as it requires more in-depth analysis of the problem and comparison with other available techniques.

The second experiment is what IIG is originally developed for. The robot explores an unknown environment; it needs to solve SLAM incrementally, estimate a dense occupancy map representation suitable

Table 1: Parameters for IIG-tree experiments. "Online" parameters are only related to the exploration experiments.

Parameter	Symbol	Value
– General parameters:		
Occupied probability	p_{occ}	0.65
Unoccupied probability	p_{free}	0.35
Initial position	x_{init}	[10,2] m
Map resolution	δ_{map}	0.2 m
I_{RIC} threshold	δ_{RIC}	5e-4
I_{RIC} threshold (Online)	δ_{RIC}	1e-2
– MI-based parameters:		
Hit std	σ_{hit}	0.05 m
Short decay	λ_{short}	0.2 m
Hit weight	z_{hit}	0.7
Short weight	z_{short}	0.1
Max weight	z_{max}	0.1
Random weight	z_{rand}	0.1
Numerical integration resolution	s_z	2 m^{-1}
Saturation probability	p_{sat}	0.05
Saturation probability (Online)	p_{sat}	0.3
Occupied belief	b_{occ}	1.66
Unoccupied belief	b_{free}	0.6
– Covariance function hyperparameters:		
characteristic length-scale	l	3.2623 m
Signal variance	σ_f^2	0.1879
– Robot motion model:		
Motion noise covariance	$\boldsymbol{Q}$	$\mathrm{diag}(0.1\,\mathrm{m}, 0.1\,\mathrm{m}, 0.0026\,\mathrm{rad})^2$
Initial pose uncertainty	$\boldsymbol{\Sigma}_{init}$	$\mathrm{diag}(0.4\,\mathrm{m}, 0.1\,\mathrm{m}, 0\,\mathrm{rad})^2$

for planning and navigation, and automatically detect the completion of an exploration mission. Therefore, the purpose of information gathering is map completion while maintaining accurate pose estimation, i.e. planning for estimation. We compare exploration experiments where the robot pose is estimated through a pose graph algorithm such as Pose SLAM (Ila et al. 2010), and the map of the unknown environment is computed using the Incremental Gaussian Processes Occupancy Mapping (I-GPOM) (Ghaffari Jadidi et al. 2014, 2016). Therefore, the state which includes the robot pose and the map is partially observable.

In the third scenario, we demonstrate another possible application of IIGs in a lake monitoring experiment using experimental data collected by an Autonomous Surface Vehicle (ASV). This dataset is also used in the original RIG paper (Hollinger and Sukhatme 2014) [11]. In the end, we also discuss the limitations of this work including our observations and conjectures. The algorithms are implemented in MATLAB and the code is publicly available [12].

[11] The dataset is available on: http://research.engr.oregonstate.edu/rdml/software

[12] https://github.com/MaaniGhaffari/sampling_based_planners

9.1 Experiments Setup

We first briefly describe the experiment setup that is used in Subsections 9.2 and 9.3. The parameters for experiments and the information functions are listed in Table 1. The environments are constructed using a binary map of obstacles. For GPVR-based algorithms, the covariance function is Matérn ($\nu = 5/2$)

$$k_{VR} = \sigma_f^2 k_{\nu=5/2}(r) = \sigma_f^2 (1 + \frac{\sqrt{5}r}{l} + \frac{5r^2}{3l^2}) \exp(-\frac{\sqrt{5}r}{l}) \tag{26}$$

with hyperparameters that were learned prior to the experiments and are available in Table 1. The modified kernel in UGPVR algorithm was calculated using Gauss-Hermite quadrature with 11 sample points. The robot pose covariance was approximated using the worst-case uncertainty propagation and local linearization of the robot motion model using Equations (15) and (16). Each run was continued until the algorithm converges without any manual intervention. In case of multiple runs for an algorithm we report the mean and the standard error of outcomes. Furthermore, in all experiments, we used unlimited budget to see the performance of each method in the limit and also examine our convergence criteria for IIG and exploration experiments (Corollary 13). The online parameters in Table 1 refer to exploration experiments and are used in Subsection 9.3.

9.2 Comparison of Information Functions

We now compare the proposed information functions by running IIG-tree using different sensor parameters. The map is initialized as an occupancy grid map by assigning each point the occupied or unoccupied probability according to its groundtruth status. For GPVR-based methods, an initial variance map is set to the value of 1 for all points. In the first experiment, we varied the number of sensor beams by running each method for 30 times. The chosen number of beams are 10, 20, and 50. The compared information functions are MI, MIUB, GPVR, and UGPVR, and the results are presented in Table 2. The maximum sensor range is kept fixed at $r_{max} = 5\,\mathrm{m}$ and the convergence is detected when the average of penalized relative information contribution I_{RIC} over a window of size 30 drops below the threshold $\delta_{RIC} = 5e-4$. The total information gain/cost are calculated using the sum of all edges information/cost. Therefore, it denotes the total information/cost over the searched space and not a particular path. The reason is to avoid any possible randomness in path selection which can make the results biased. In other words, the results are independent of the path selection algorithm.

From Table 2, MIUB has the lowest runtime which is expected, followed by MI, GPVR, and UGPVR, respectively. However, MI has the fastest convergence speed with, approximately, half of the number of samples taken by GPVR. The calculation of MI can be more expensive than GPVR-based algorithms, but using sparse sensor observations (only 10 beams) and a very coarse numerical integration resolution it performs faster. For all the compared algorithms, as the number of beams increases, i.e. taking more observations, the computational time rises, and the number of samples/nodes reduces. An important observation is that incorporating the pose uncertainty in UGPVR leads to a slower convergence. This can

Table 2: Comparison of the information functions in offline IIG-tree experiments by increasing the sensor number of beams from 10 to 50. The figures are averaged over 30 experiments (mean ± standard error). For all experiments the following parameters are set in common $r_{max} = 5\,\text{m}$, $\delta_{RIC} = 5e-4$.

Number of beams n_z	10	20	50
Mutual information (MI)			
Planning time (min)	6.88 ± 0.16	8.44 ± 0.27	14.64 ± 0.81
Number of samples	911 ± 19	588 ± 13	435 ± 20
Number of nodes	402 ± 5	280 ± 5	181 ± 8
Total information gain (NATS)	1.4071e+04 ± 148.3	1.3624e+04 ± 173.8	1.2546e+04 ± 313.2
Total cost (m)	336.3 ± 3.8	258.5 ± 3.7	187.2 ± 7.7
Mutual information upper bound (MIUB)			
Planning time (min)	4.53 ± 0.16	6.95 ± 0.28	12.88 ± 0.51
Number of samples	1014 ± 24	629 ± 17	486 ± 15
Number of nodes	444 ± 8	303 ± 7	212 ± 5
Total information gain (NATS)	2.0472e+04 ± 169.2	1.9602e+04 ± 207.7	1.9881e+04 ± 403.1
Total cost (m)	358.3 ± 5.6	272.0 ± 5.0	211.5 ± 4.4
GP variance reduction (GPVR)			
Planning time (min)	9.31 ± 0.39	13.10 ± 0.41	15.07 ± 0.61
Number of samples	1677 ± 53	1135 ± 36	874 ± 36
Number of nodes	616 ± 15	477 ± 13	382 ± 11
Total information gain (NATS)	7840.6 ± 62.8	9123.4 ± 80.5	1.3111e+04 ± 176.9
Total cost (m)	490.5 ± 9.5	392.4 ± 7.9	320.6 ± 7.2
Uncertain GP variance reduction (UGPVR)			
Planning time (min)	19.75 ± 0.48	27.89 ± 0.94	47.79 ± 2.16
Number of samples	4746 ± 136	2633 ± 102	1828 ± 81
Number of nodes	1344 ± 28	913 ± 25	704 ± 22
Total information gain (NATS)	3197.6 ± 16.0	3731.3 ± 22.1	5557.5 ± 52.4
Total cost (m)	894.0 ± 16.3	621.4 ± 15.6	497.8 ± 12.5

be explained as a result of the reduction in the information content of each set of observations by adding uncertainty to the information gain calculation. Another interpretation is that the UGPVR algorithm is, relatively speaking, less greedy or more conservative for information gathering. MI in comparison to MIUB has more realistic information gain estimation which is reflected in less total cost on average. The latter results also confirm the advantage of maximizing the information gain rather than minimizing the entropy which is discussed in Krause et al. (2008).

In the second experiment, the number of beams is kept fixed at $n_z = 10$, but the sensor range is increased from 5 m to 20 m. The results shown in Table 3 are consistent with the previous test and the variations are even slighter. In fact, the first column of Table 3 is the repetition of the experiment with the similar parameters to the first column of Table 2, for another 30 runs [13]. Furthermore, the difference between $r_{max} = 10$ and $r_{max} = 20$ cases is marginal which shows increasing the sensor range more than

[13] The results are computed during several days using high-performance computing facilities at the University of Technology Sydney and the reported time is affected by other users activities. However, it can be used for relative comparison and other factors remain consistent.

Table 3: Comparison of the information functions in offline IIG-tree experiments by increasing the sensor range from 5 m to 20 m (averaged over 30 experiments, mean ± standard error). For all experiments the following parameters are set in common $n_z = 10$; $\delta_{RIC} = 5e-4$.

Sensor range r_{max} (m)	5	10	20
Mutual information (MI)			
Planning time (min)	5.00 ± 0.13	6.60 ± 0.10	7.88 ± 0.11
Number of samples	979 ± 22	782 ± 21	780 ± 20
Number of nodes	423 ± 7	352 ± 8	360 ± 6
Total information gain (NATS)	1.4019e+04 ± 146.5	1.4525e+04 ± 177.9	1.5789e+04 ± 220.9
Total cost (m)	351.7 ± 4.8	307.8 ± 5.4	309.2 ± 4.0
Mutual information upper bound (MIUB)			
Planning time (min)	3.67 ± 0.10	3.56 ± 0.08	3.87 ± 0.11
Number of samples	1015 ± 23	813 ± 15	811 ± 20
Number of nodes	444 ± 7	368 ± 6	369 ± 7
Total information gain (NATS)	2.0414e+04 ± 161.7	1.9845e+04 ± 228.5	1.9730e+04 ± 272.9
Total cost (m)	360.1 ± 5.2	309.9 ± 4.2	311.6 ± 4.5
GP variance reduction (GPVR)			
Planning time (min)	6.20 ± 0.22	7.03 ± 0.24	6.60 ± 0.22
Number of samples	1745 ± 71	1393 ± 41	1248 ± 48
Number of nodes	636 ± 18	559 ± 13	523 ± 16
Total information gain (NATS)	7977.7 ± 56.4	7801.6 ± 71.0	7835.1 ± 62.5
Total cost (m)	501.7 ± 11.2	445.0 ± 7.5	422.7 ± 9.8
Uncertain GP variance reduction (UGPVR)			
Planning time (min)	20.52 ± 0.65	26.3 ± 0.68	26.68 ± 0.54
Number of samples	4994 ± 167	3661 ± 109	3385 ± 87
Number of nodes	1404 ± 35	1139 ± 25	1078 ± 19
Total information gain (NATS)	3174.8 ± 19.3	3254.2 ± 21.4	3271.0 ± 21.0
Total cost (m)	934.4 ± 22.3	765.2 ± 15.5	724.1 ± 12.3

10 m does not improve the information gathering process in this environment. Overall, we can conclude that by changing the parameters the convergence of IIG using the relative information contribution notion remains consistent, and the speed of convergence varies reasonably with the parameters. We reiterate that the $\delta_{RIC} = 5e-4$ is used for all the results in Table 2 and 3 and this demonstrates a strong correlation with the planning time (horizon) for each information function, by ignoring the overhead computations due to the increase in n_z or r_{max}.

In Figure 3, an example of IIG-tree using MI information function in the Cave map (Howard and Roy 2003) is illustrated. The sensor range and the number of beams are set to 5 m and 10, respectively. Figure 3a shows the map of the environment, Figure 3b illustrates the IIG graph where the extracted paths are also shown and the most informative path is separated using a darker color. The convergence of I_{RIC} for both MI and MIUB is shown in Figure 3c, and Figure 3d shows the calculated information gain in NATS where its diminishing return over time (as the number of samples grows) is evident.

The equivalent results for IIG-tree using GPVR and UGPVR information functions are shown in Figure 4 and Figure 5. It is interesting to observe that I_{RIC} converges to close values for MIUB and GPVR, but

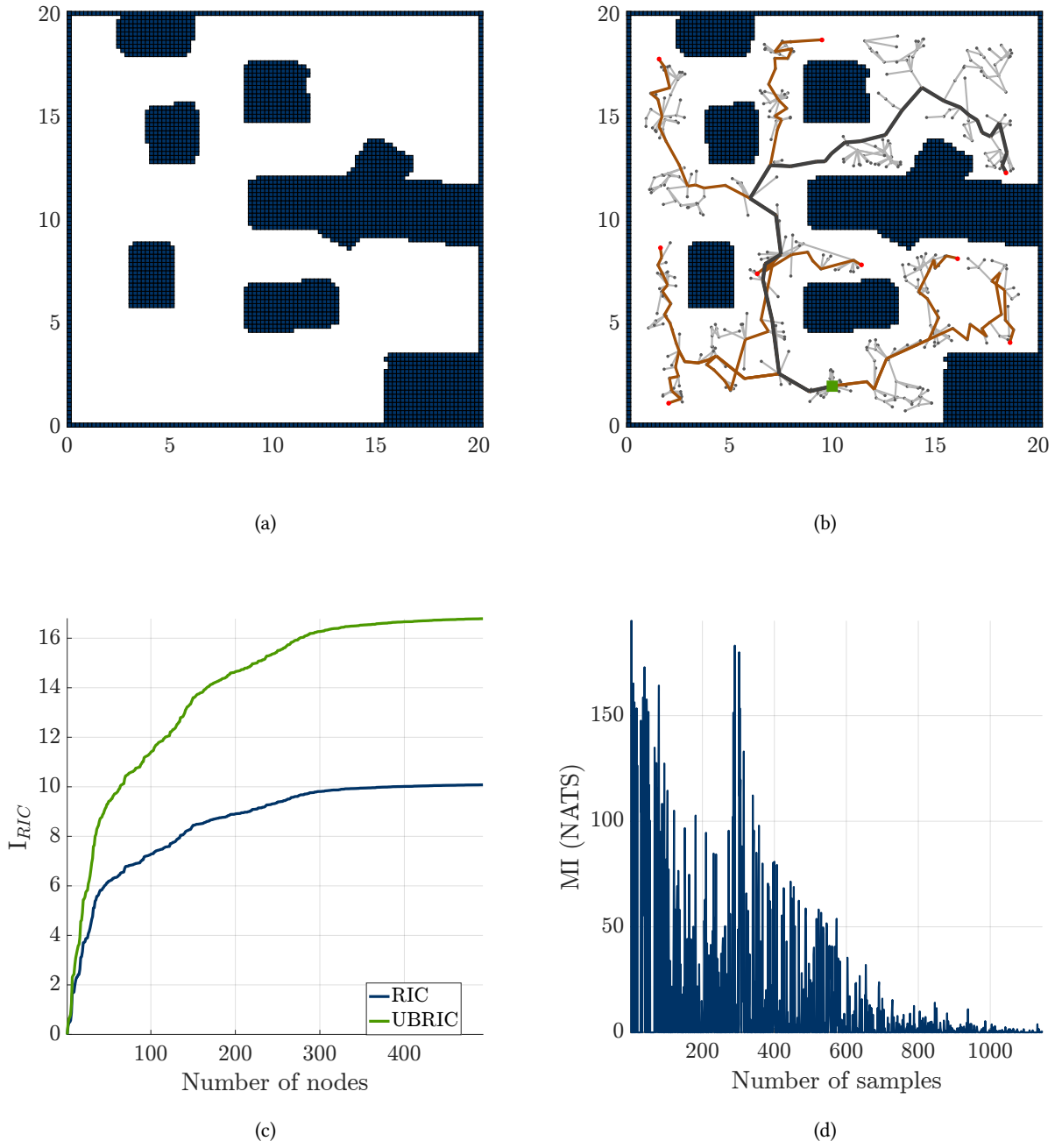

Figure 3: Results from running the IIG-tree algorithm using MI information function in the Cave map. (a) shows the map of the environment. (b) shows the IIG-tree graph and the selected paths, the most informative path is shown using a darker color. (c) is the convergence graph of the penalized relative information contribution I_{RIC} for MI and MIUB. (d) shows the evolution of the information gain calculation.

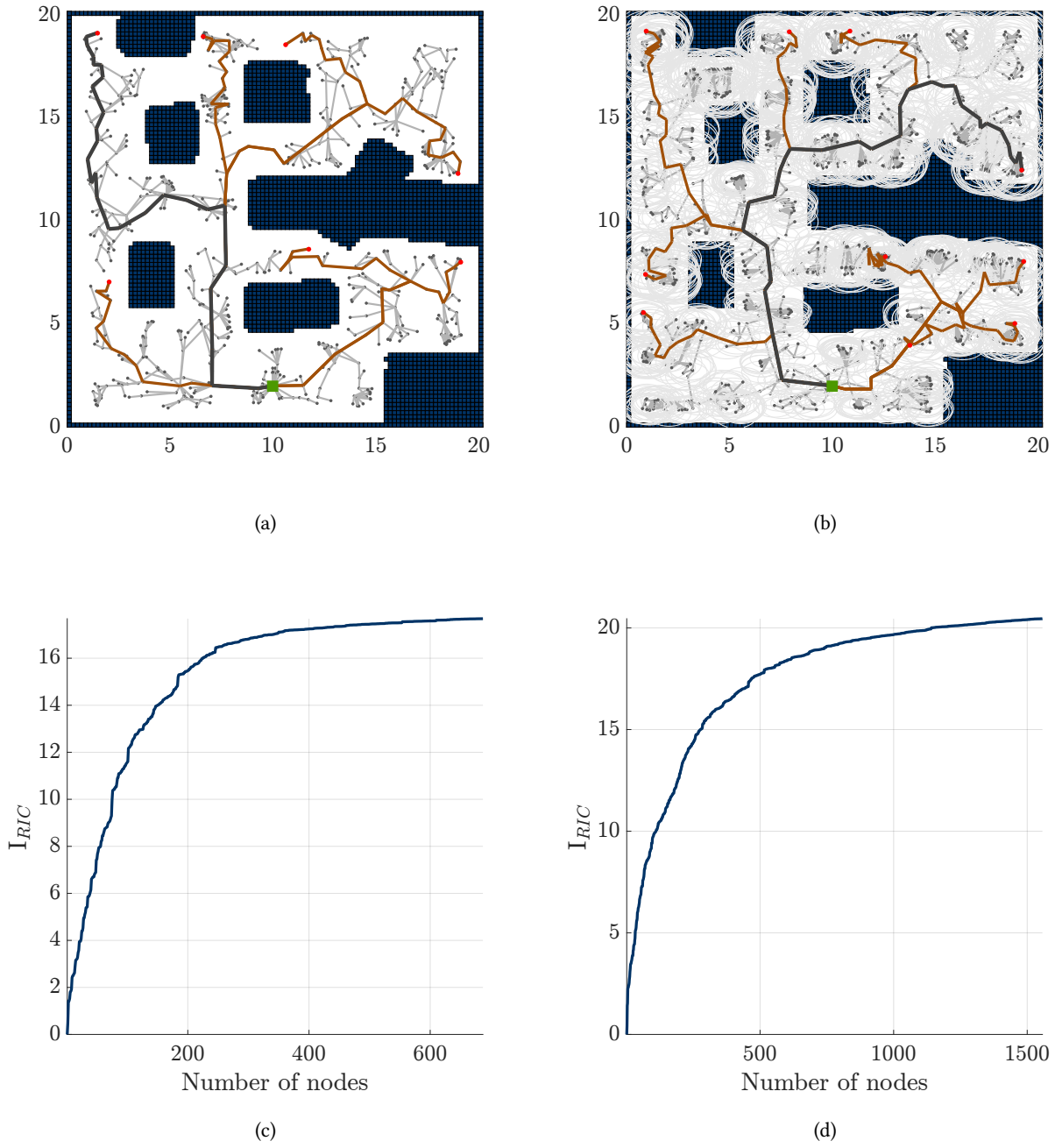

Figure 4: Results from running the IIG-tree algorithm using GPVR and UGPVR information functions in the Cave map. IIG-tree graph and the selected paths for (a) using GPVR information function, and (b) using UGPVR information function. The most informative path is shown using a darker color. The convergence graph of the penalized relative information contribution I_{RIC} for (c) GPVR, and (d) UGPVR.

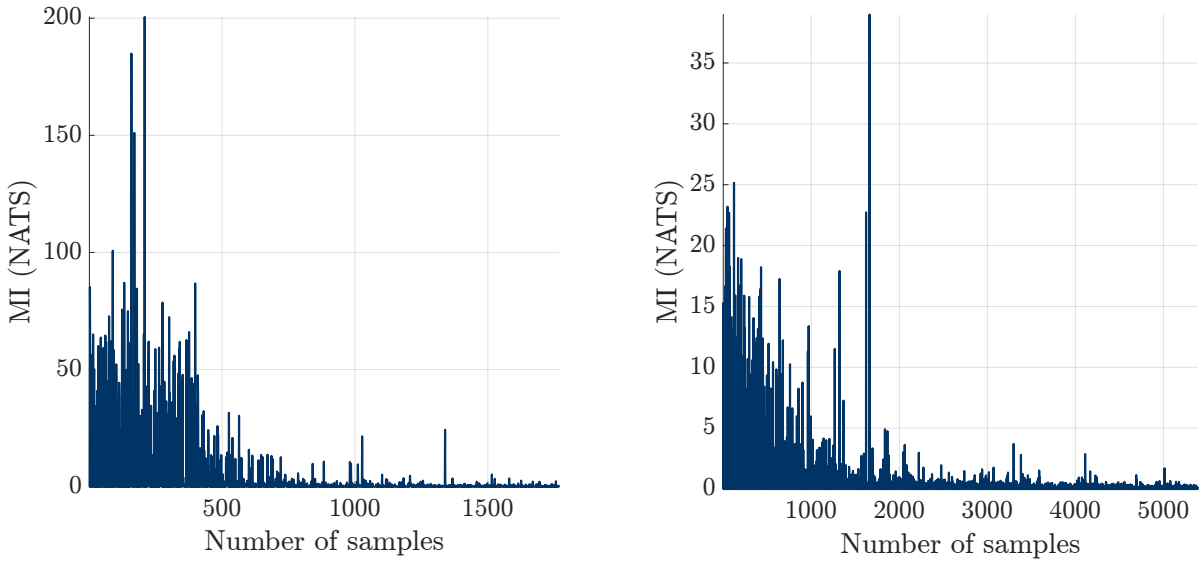

(a) (b)

Figure 5: Evolution of the information gain calculation for (a) IIG-tree using GPVR information function, and (b) IIG-tree using UGPVR information function.

it has a lower value for MI as the estimated information gain is more realistic by taking the expectation over future measurements. For UGPVR information function, we can see that I_{RIC} is increased. From Figure 4d and Figure 5b, we can conclude that the overall trend is similar to the GPVR case. However, due to the incorporated pose uncertainty the amount of information gain is remarkably lower which explains the longer tail of information gain evolution before the convergence of the algorithm and the higher relative information contribution from each node. In other words, farther nodes have higher pose uncertainties. Therefore the discrimination between farther and nearer nodes from relative information contribution is less than the case where the pose uncertainty is ignored.

Finally, a practical conclusion can be that increasing the sensor range and the number of beams (observations) increases the computational time but does not necessarily make the corresponding information function superior to its coarser approximation. As long as the approximation can capture the essence of information gain estimation consistently, the search algorithm performs well. However, we should acknowledge that the conclusion is not complete, and the structural shape of the environment affects the result, e.g. the maximum and minimum perception field at different areas of the map. We use these results to select a sensor configuration for the next experiments. To speed up the exploration scenario, we select $n_z = 10$ and $r_{max} = 5\,\mathrm{m}$ which lead to the fastest computational time with reasonable total information gain and cost values.

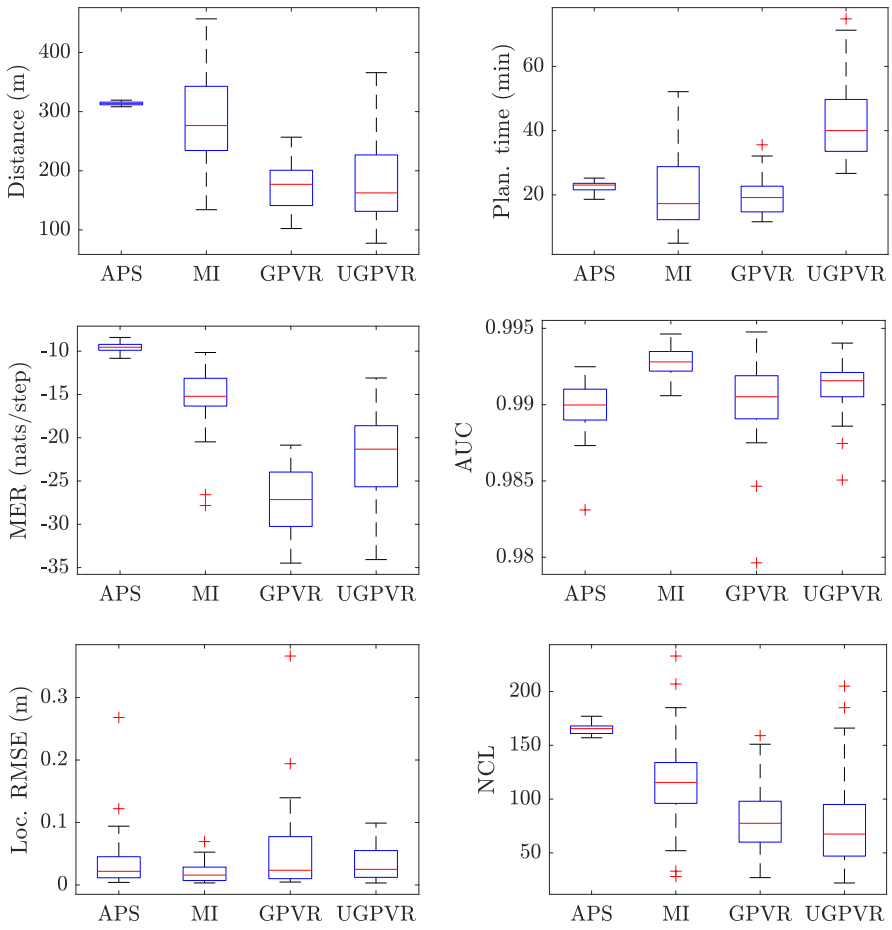

Figure 6: The box plots show the statistical summary of the comparison of different exploration strategies in the Cave dataset. The compared methods are APS, IIG-MI, IIG-GPVR, and IIG-UGPVR.

9.3 Robotic Exploration in Unknown Environments

In this section, we examine the proposed algorithms in the interesting and challenging scenario of autonomous robotic exploration in an unknown map. The robot does not have any prior information neither from the map nor its location. Therefore, it needs to solve the SLAM problem for localization and possibly the topological map of features (environment). Then building a dense map representation that shows occupied and unoccupied regions for planning and navigation. The robot pose and map are partially observable which makes the planning for a long horizon difficult. We solve the localization problem using Pose SLAM, the occupancy mapping using I-GPOM, and the planning using IIG-tree with different information functions for comparison. We also compare our results with Active Pose SLAM (APS) (Valencia et al. 2012) which is an information gain-based technique that considers explicit loop-closures by searching through nearby poses in the pose graph. APS uses an OGM for mapping and exploration. Pose SLAM parameters were set and fixed regardless of the exploration method. The localization root mean square error (RMSE) was computed at the end of each experiment by the difference in the robot esti-

mated and ground truth poses. The occupancy maps are compared using the area under the receiver operating characteristic curve (AUC). The probability that the classifier ranks a randomly chosen positive instance higher than a randomly chosen negative instance can be understood using the AUC of the classifier (Fawcett 2006).

Figure 6 shows the statistical summary of the results from exploration experiments in the Cave environment. The results are from 30 exploration rounds in which each mission was terminated automatically using Corollary 13 and saturation probability $p_{sat} = 0.1$ [14]. The IIG-GPVR has the lowest travel distance, highest map entropy reduction rate, but, relatively speaking, the highest localization error. The improvement in the map entropy rate over our previous results on the same dataset using MI-based greedy exploration (Ghaffari Jadidi et al. 2015) is roughly more than 1.63 times which is surprisingly high for an algorithm that can preserve the localization accuracy better as well. IIG-UGPVR demonstrates a more conservative version of IIG-GPVR which by more planning time due to the pose uncertainty propagation provides better localization and map accuracies. This behavior is expected and shows the consistency between our problem definition and algorithmic development.

From another point of view, IIG-MI has the lowest localization error with a similar planning time, but higher travel distance. The IIG-MI makes direct use of sensor model for information gain estimation. The fact that the sensor model for range-finders is an accurate model together with the correlation between the map and robot pose leads to implicit pose uncertainty reduction. This result reveals the fundamental difference between mutual information approximation using a direct method (taking the expectation over future measurements) and GP which to best of our knowledge was not previously discussed in the literature.

9.4 Lake Monitoring Experiment

In this experiment, we demonstrate the performance of IIGs in a lake monitoring scenario. The ASV can localize using a GPS unit and a Doppler Velocity Log. The communication with the ground station is through a 802.11 wireless connection and at any location the wireless signal strength (WSS) can be measured in dBm. The Puddingstone Lake dataset is a publicly available dataset that includes about 2700 observations. The dataset is collected through a full survey of the lake area located at Puddingstone Lake in San Dimas, CA (Lat. 34.088854°, Lon. -117.810667°) (Hollinger and Sukhatme 2014). The objective is to find a trajectory for the robot to maintain a strong connectivity with the base station while taking physical samples in the lake.

The groundtruth map of WSS is built using GP regression with a constant mean function, SE covariance function with automatic relevance determination (ARD) (Neal 1996), and a Gaussian likelihood function which makes the exact inference possible. Furthermore, it is well-known that, in line of sight scenarios, radio signals propagation can be characterized based on Friis free space model (Rappaport 1996;

[14] Note that MI-based information functions and map exploration termination condition have different saturation probabilities that do not necessarily have a similar value.

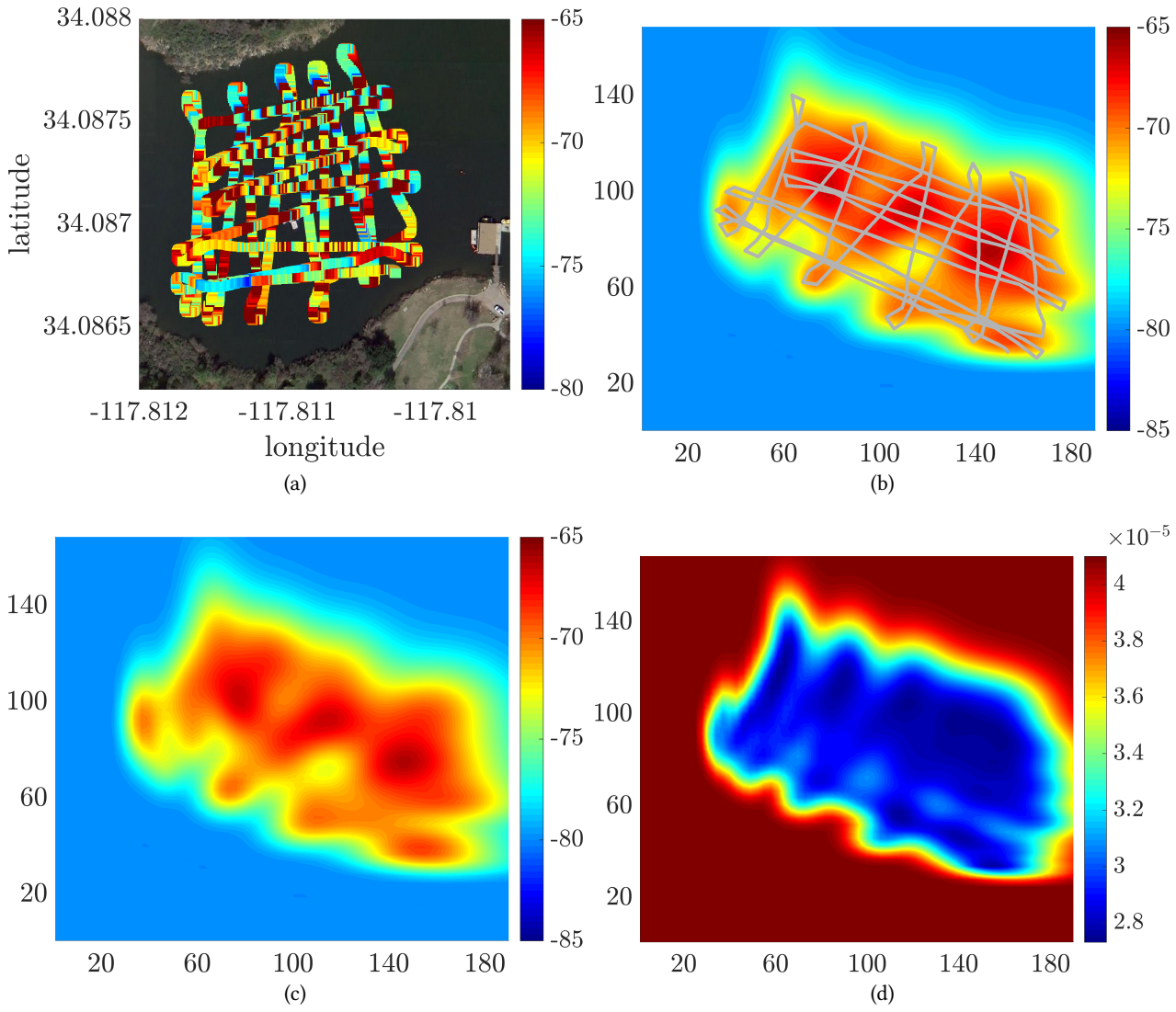

Figure 7: Lake monitoring scenario (a) satellite view of the lake and the survey trajectories using ASV, (b) the robot trajectories in metric scale on WSS map, (c) GP WSS mean surface (in dBm), and (d) GP WSS covariance surface.

Goldsmith 2005). In this model, the signal attenuation is proportional to the logarithm of the distance. Therefore, to improve the regression accuracy we use logarithmic scales for input points during GP training and inference phases. The number of training points was down-sampled to 267 observations and the surface was inferred using 3648 query points. We store the output using a kd-tree data structure to be able to perform fast online nearest neighbor inquiries within the robot sensing range. Figure 7 shows the satellite view of the lake area together with the survey trajectories and regressed maps that are used as a proxy for groundtruth. Figure 7b shows the survey trajectories on the WSS surface where the longitudes and latitudes are converted to their corresponding distances using the haversine formula. Figures 7c and 7d illustrate the GP WSS mean and covariance surfaces, respectively.

Table 4: Lake monitoring experiments using IIG with GPVR and UGPVR information functions. For the comparison, the sensing range is varied from 5 m to 20 m. The results are averaged over 100 runs (mean ± standard error). For all experiments $\delta_{RIC} = 5e-4$.

Sensor range (m)	5	10	15	20
		IIG-GPVR		
Time (sec)	5.26 ± 0.16	2.92 ± 0.08	2.38 ± 0.09	2.32 ± 0.07
RMSE (dBm)	4.54 ± 0.05	4.28 ± 0.06	3.97 ± 0.06	3.61 ± 0.07
Number of samples	830.6 ± 18.7	507.9 ± 13.0	437.0 ± 15.6	428.1 ± 12.9
Number of nodes	826.1 ± 18.7	454.5 ± 12.8	359.9 ± 14.5	331.6 ± 12.7
Total information gain (NATS)	2.0817e+04 ± 160.1	2.4272e+04 ± 111.2	2.6207e+04 ± 133.1	2.7716e+04 ± 130.6
Total cost (Km)	6.77 ± 0.11	4.50 ± 0.09	3.67 ± 0.11	3.42 ± 0.10
		IIG-UGPVR		
Time (sec)	33.98 ± 1.30	25.93 ± 0.67	29.26 ± 0.98	53.69 ± 1.61
RMSE (dBm)	4.55 ± 0.05	4.26 ± 0.05	4.00 ± 0.06	3.56 ± 0.07
Number of samples	844.8 ± 19.8	496.0 ± 12.3	467.4 ± 15.4	413.0 ± 13.3
Number of nodes	839.2 ± 19.7	447.9 ± 12.4	389.1 ± 14.9	325.8 ± 12.8
Total information gain (NATS)	2.1268e+04 ± 176.7	2.4967e+04 ± 107.8	2.6925e+04 ± 120.6	2.8087e+04 ± 113.9
Total cost (Km)	6.81 ± 0.13	4.46 ± 0.09	3.91 ± 0.11	3.39 ± 0.10

For information functions, we used Algorithms 6 and 7 as they are natural choices for scenarios involving spatial phenomenas and environmental monitoring. The experiment is designed in such a way that at any location the robot can take measurements within a sensing range from the grundtruth maps. This step replaces the raytracing operation in both algorithms. The modified kernel in Algorithm 7 was calculated using Gauss-Hermite quadrature with 11 sample points. The robot pose covariance was approximated using the worst-case uncertainty propagation and local linearization of the robot motion model [15]. Table 4 shows the comparison results between IIG-GPVR and IIG-UGPVR using several criteria including RMSE. To calculate the RMSE, we used the collected measurements along the most informative path extracted from the IIG graph using Algorithm 8 and rebuilt the GP WSS mean surface with the same resolution. We repeated the experiment 100 times with 5 m, 10 m, 15 m, and 20 m sensing ranges. The IIG-GPVR algorithm is faster and can compute the most informative trajectory in only a few seconds. This is promising for online applications where the robot needs to replan along the trajectory. Note that, as it is expected, by increasing the sensing range, the information gain rises and the total cost and RMSE decrease. However, this means it is assumed that in reality the signal strength at any location has stronger correlations with its nearby locations. While this is true for the presented experiment, in a cluttered environment, it can be an unrealistic assumption.

Figure 8 shows the illustrative examples of IIG-GPVR with different sensing ranges. As the sensing range increases, the graph becomes gradually sparser. This can be understood from the fact that the information from a larger neighborhood is integrated into each node. Note that the objective is to explore the entire area while maintaining a strong wireless connectivity with the based station, therefore, the robot does not need to always travel in the area with high signal strengths. However, it travels most of

[15] The pose uncertainties are not part of the original dataset. Hence, we calculate them by simulation.

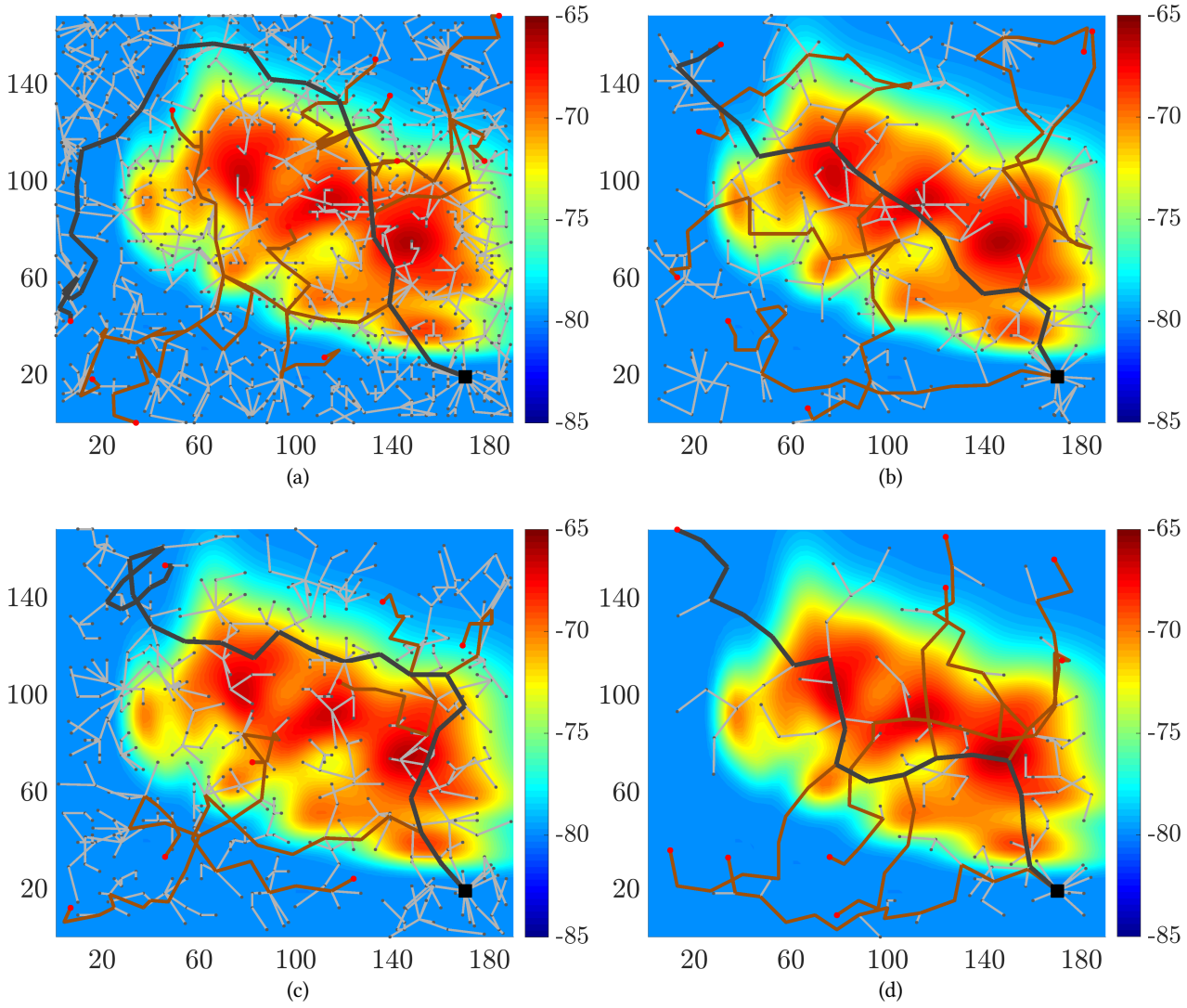

Figure 8: Informative motion planning for WSS monitoring in the lake area using IIG-GPVR with sensing range (a) 5 m (b) 10 m (c) 15 m, and (d) 20 m.

the time in the areas with strong connectivity. Figure 9 shows the same scenario using IIG-UGPVR. The main difference is that the robot behaves more conservatively and tends to return to the regions with strong connectivity. The growth in pose uncertainty by traveling farther, reduces the information gain of those areas. In both IIG-GPVR and IIG-UGPVR results, we can see that by increasing the sensing range the robot tends to explore farther distances which is a natural behavior, in Figures 8d and 9d.

9.5 Limitations and Observations

The proposed algorithms can provide an approximate solution to the robotic exploration problem in unknown environments as a basic navigation task as well as environmental monitoring tasks. Although IIG

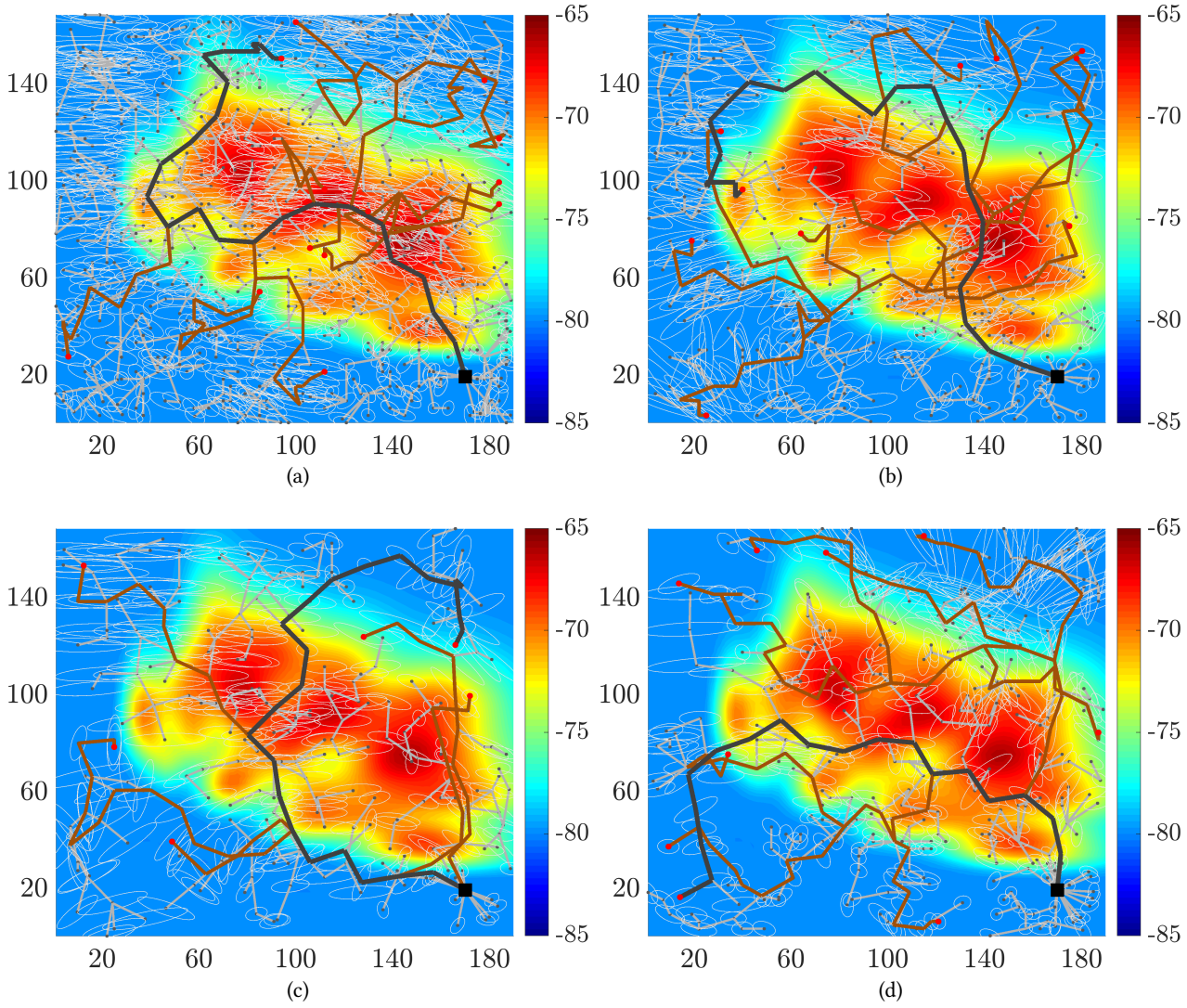

Figure 9: Informative motion planning for WSS monitoring in the lake area using IIG-UGPVR with sensing range (a) 5 m (b) 10 m (c) 15 m, and (d) 20 m. By incorporating pose uncertainties in planning, the informative trajectories are those in which not only the wireless connectivity is strong, but the pose uncertainty along the trajectories is minimized.

can be implemented for online tasks, it has the limitations of its ancestors. Therefore, violating the main assumptions, such as availability of free area near any point for graph expansion, can result in failure of the task. More conceptually, most of the present robotic navigation algorithms are not truly adaptive as they commit to a decision once it is planned and replanning occurs only if the amount of computation is manageable, and often not with a high frequency. So there will be a window of time the robot acts based on the previously made decision. Although humans act in a similar fashion, we can make decisions more spontaneously (fully adaptive). This problem can be severe in environments that are highly dynamic as the robot is not as responsive as it is required.

To our experience, using a coarse approximation, i.e. less number of beams than the actual range-

finder sensor results in not only faster search in the workspace and reducing the computational time, but giving the chance to more samples to be candidates as part of the potential most informative path. This is a promising feature that the algorithm works reasonably well without near exact estimation of information quality. Moreover, uniform sampling produces reasonable results in the early stage, however as the graph grows, this sampling strategy becomes less efficient. Biasing the sampling towards directions that are less explored may lead to a faster convergence.

10 Conclusion and Future Work

In this work, we developed a sampling-based planning algorithm for incremental robotic information gathering. The proposed algorithm is based on RIG and offers an information-theoretic convergence criterion using the notion of penalized relative information contribution. We formulated the problem as an information maximization problem subject to budget and state estimate constraints. The unique feature of this approach is that it can handle dense belief representations as well as the robot pose uncertainty. We proposed MI-based and GPVR-based information functions and their variants that can be used in both RIG and IIG frameworks. The proposed IIG-tree algorithm using a UGPVR information function considers pose uncertainties in planning and provides an approximate solution for finding maximally informative paths under partially observable state variables.

The proposed algorithms can directly be applied to environmental monitoring and robotic exploration tasks in unknown environments. The proposed algorithms have also potential applications in solving the sensor configuration selection problem that we did not fully investigate as it is beyond the scope of this work. Furthermore, the planning horizon does not need to be set as a number of steps. Instead, the information-theoretic representation of the planning horizon used here brings more flexibility for managing the convergence of the algorithm.

We would like to share some ideas that are natural extensions of this work. For the sake of clarity, we itemize them as follows.

(i) The algorithms in this article could be extended for multi-robot planning; exploiting the information gain available through wireless communication channels to manage the coordination between robots while a feedback controller satisfied kinodynamic constraints.

(ii) We developed IIG-tree based on the RIG-tree algorithm. IIG could also be used to extend RIG-roadmap and RIG-graph. RIG-graph is asymptotically optimal and can asymptotically explore all possible budget-constraint trajectories, it produces a fully connected graph and is an interesting case to study. Therefore, IIG-graph would allow us to generate a unique trajectory without choosing one from several, reducing the number steps required for incremental planning tasks such as robotic exploration.

(iii) While we provide a procedural implementation of the proposed algorithms, and it suffices for re-

search and comparison purposes, we believe the integration of the algorithms in open source libraries such as the Open Motion Planning Library (OMPL) (Sucan et al. 2012) has advantages for possible applications of this work.

(iv) The GPVR-based algorithms could be used for active learning to model the quantity of interest online using GPs.

(v) IIG/RIG frameworks could be used for maximizing a multi-objective information function to perform multiple tasks concurrently. In a naïve approach, the objective function can be defined as the sum of information functions; however, if random variables from different information functions are correlated, e.g. through the robot pose, the total information gain calculation will not be accurate. Hence, developing a more systematic approach is an interesting avenue to follow.

(vi) A sparse covariance matrix could be constructed using the Sparse covariance function. Exploiting the sparse structure of the covariance matrix for large-scale problems could be an interesting extension of this work for online implementations.

References

Agha-mohammadi Aa, Chakravorty S and Amato NM (2014) FIRM: Sampling-based feedback motion-planning under motion uncertainty and imperfect measurements. *The Int. J. Robot. Res.* 33(2): 268–304. 4

Astrom K (1965) Optimal control of Markov processes with incomplete state information. *Journal of Mathematical Analysis and Applications* 10(1): 174–205. 4

Bertsekas DP (1995) *Dynamic programming and optimal control*, volume 1. Athena Scientific Belmont, MA. 4

Binney J, Krause A and Sukhatme GS (2013) Optimizing waypoints for monitoring spatiotemporal phenomena. *The Int. J. Robot. Res.* 32(8): 873–888. 3, 4, 5, 20

Binney J and Sukhatme GS (2012) Branch and bound for informative path planning. In: *Proc. IEEE Int. Conf. Robot Automat.* IEEE, pp. 2147–2154. 3, 5, 12

Bry A and Roy N (2011) Rapidly-exploring random belief trees for motion planning under uncertainty. In: *Proc. IEEE Int. Conf. Robot Automat.* IEEE, pp. 723–730. 4, 11

Cover TM and Thomas JA (1991) *Elements of information theory*. John Wiley & Sons. 6, 7, 21

Davis PJ and Rabinowitz P (1984) *Methods of numerical integration*. Academic Press. 22

Dhariwal A, Sukhatme GS and Requicha AA (2004) Bacterium-inspired robots for environmental monitoring. In: *Proc. IEEE Int. Conf. Robot Automat.*, volume 2. IEEE, pp. 1436–1443. 3

Dunbabin M and Marques L (2012) Robots for environmental monitoring: Significant advancements and applications. *IEEE Robotics & Automation Magazine* 19(1): 24–39. 3

Fawcett T (2006) An introduction to ROC analysis. *Pattern recognition letters* 27(8): 861–874. 35

Ghaffari Jadidi M, Miro JV, Valencia R and Andrade-Cetto J (2014) Exploration on continuous Gaussian process frontier maps. In: *Proc. IEEE Int. Conf. Robot Automat.* pp. 6077–6082. 10, 27

Ghaffari Jadidi M, Valls Miro J and Dissanayake G (2015) Mutual information-based exploration on continuous occupancy maps. In: *Proc. IEEE/RSJ Int. Conf. Intell. Robots Syst.* pp. 6086–6092. 17, 35

Ghaffari Jadidi M, Valls Miro J and Dissanayake G (2016) Gaussian process autonomous mapping and exploration for range sensing mobile robots. *arXiv preprint arXiv:1605.00335* . 17, 27

Ghaffari Jadidi M, Valls Miro J, Valencia Carreño R, Andrade-Cetto J and Dissanayake G (2013) Exploration in information distribution maps. In: *RSS Workshop on Robotic Exploration, Monitoring, and Information Content.* 10

Goldsmith A (2005) *Wireless communications*. Cambridge university press. 36

Guestrin C, Krause A and Singh AP (2005) Near-optimal sensor placements in Gaussian processes. In: *Proceedings of the 22nd international conference on Machine learning*. ACM, pp. 265–272. 20

Hollinger GA (2015) Long-horizon robotic search and classification using sampling-based motion planning. In: *Robotics: Science and Systems*. 5

Hollinger GA and Sukhatme GS (2013) Sampling-based motion planning for robotic information gathering. In: *Robotics: Science and Systems*. 3, 5

Hollinger GA and Sukhatme GS (2014) Sampling-based robotic information gathering algorithms. *The Int. J. Robot. Res.* 33(9): 1271–1287. 3, 5, 10, 11, 12, 27, 35

Horsch T, Schwarz F and Tolle H (1994) Motion planning with many degrees of freedom-random reflections at c-space obstacles. In: *Proc. IEEE Int. Conf. Robot Automat.* IEEE, pp. 3318–3323. 4

Howard A and Roy N (2003) The robotics data set repository (Radish). URL http://radish.sourceforge.net. 30

Huynh VA and Roy N (2009) icLQG: combining local and global optimization for control in information space. In: *Proc. IEEE Int. Conf. Robot Automat.* IEEE, pp. 2851–2858. 4

Ila V, Porta J and Andrade-Cetto J (2010) Information-based compact Pose SLAM. *IEEE Trans. Robot.* 26(1): 78–93. 27

Indelman V, Carlone L and Dellaert F (2015) Planning in the continuous domain: A generalized belief space approach for autonomous navigation in unknown environments. *The Int. J. Robot. Res.* 34(7): 849–882. 4

Kaelbling LP, Littman ML and Cassandra AR (1998) Planning and acting in partially observable stochastic domains. *Artificial intelligence* 101(1): 99–134. 4

Karaman S and Frazzoli E (2011) Sampling-based algorithms for optimal motion planning. *The Int. J. Robot. Res.* 30(7): 846–894. 4, 11, 12

Kavraki LE, Švestka P, Latombe JC and Overmars MH (1996) Probabilistic roadmaps for path planning in high-dimensional configuration spaces. *Robotics and Automation, IEEE Transactions on* 12(4): 566–580. 4

Kim A and Eustice RM (2015) Active visual slam for robotic area coverage: Theory and experiment. *The Int. J. Robot. Res.* 34(4-5): 457–475. 3

Kim S and Kim J (2013) Occupancy mapping and surface reconstruction using local Gaussian processes with kinect sensors. *IEEE Transactions on Cybernetics* 43(5): 1335–1346. 10

Kim S and Kim J (2015) GPmap: A unified framework for robotic mapping based on sparse Gaussian processes. In: *Field and Service Robotics*. Springer, pp. 319–332. 10

Krause A, Singh A and Guestrin C (2008) Near-optimal sensor placements in Gaussian processes: Theory, efficient algorithms and empirical studies. *The Journal of Machine Learning Research* 9: 235–284. 8, 20, 29

Kurniawati H, Du Y, Hsu D and Lee WS (2011) Motion planning under uncertainty for robotic tasks with long time horizons. *The Int. J. Robot. Res.* 30(3): 308–323. 4

Kurniawati H, Hsu D and Lee WS (2008) Sarsop: Efficient point-based POMDP planning by approximating optimally reachable belief spaces. In: *Robotics: Science and Systems*. 4

Lan X and Schwager M (2013) Planning periodic persistent monitoring trajectories for sensing robots in Gaussian random fields. In: *Proc. IEEE Int. Conf. Robot Automat.* IEEE, pp. 2415–2420. 3, 4

Latombe JC (1991) *Robot motion planning*, volume 124. Springer US. 4

LaValle SM (2006) *Planning algorithms*. Cambridge university press. 4

LaValle SM and Kuffner JJ (2001) Randomized kinodynamic planning. *The Int. J. Robot. Res.* 20(5): 378–400. 4

Levine DS (2010) *Information-rich path planning under general constraints using rapidly-exploring random trees*. Master's Thesis, Massachusetts Institute of Technology. 5

Marchant R and Ramos F (2012) Bayesian optimisation for intelligent environmental monitoring. In: *Proc. IEEE/RSJ Int. Conf. Intell. Robots Syst.* IEEE, pp. 2242–2249. 3

Melkumyan A and Ramos F (2009) A sparse covariance function for exact Gaussian process inference in large datasets. In: *IJCAI*, volume 9. pp. 1936–1942. 10, 21

Neal RM (1996) *Bayesian learning for neural networks*, volume 118. Springer New York. 35

Platt Jr R, Tedrake R, Kaelbling L and Lozano-Perez T (2010) Belief space planning assuming maximum likelihood observations. In: *Robotics: Science and Systems*. 4, 5

Prentice S and Roy N (2009) The belief roadmap: Efficient planning in belief space by factoring the covariance. *The Int. J. Robot. Res.* 28(11-12): 1448–1465. 4

Press WH, Teukolsky SA, Vetterling WT and Flannery BP (1996) *Numerical recipes in C*, volume 2. Cambridge university press Cambridge. 22

Pukelsheim F (2006) *Optimal design of experiments*. Society for Industrial and Applied Mathematics. 21

Rappaport TS (1996) *Wireless communications: principles and practice*, volume 2. Prentice Hall PTR New Jersey. 35

Rasmussen C and Williams C (2006) *Gaussian processes for machine learning*, volume 1. MIT press. 8

Singh A, Krause A, Guestrin C and Kaiser WJ (2009) Efficient informative sensing using multiple robots. *Journal of Artificial Intelligence Research* : 707–755. 3, 5, 12

Singh A, Ramos F, Whyte HD and Kaiser WJ (2010) Modeling and decision making in spatio-temporal processes for environmental surveillance. In: *Proc. IEEE Int. Conf. Robot Automat.* IEEE, pp. 5490–5497. 3

Smallwood RD and Sondik EJ (1973) The optimal control of partially observable Markov processes over a finite horizon. *Operations Research* 21(5): 1071–1088. 4

Stein M (1999) *Interpolation of spatial data: some theory for kriging*. Springer Verlag. 10

Ström DP, Nenci F and Stachniss C (2015) Predictive exploration considering previously mapped environments. In: *Proc. IEEE Int. Conf. Robot Automat.* IEEE, pp. 2761–2766. 3

Sucan IA, Moll M and Kavraki LE (2012) The open motion planning library. *IEEE Robotics & Automation Magazine* 19(4): 72–82. 41

Tresp V (2000) A Bayesian committee machine. *Neural Computation* 12(11): 2719–2741. 21

Valencia R, Morta M, Andrade-Cetto J and Porta JM (2013) Planning reliable paths with Pose SLAM. *IEEE Trans. Robot.* 29(4): 1050–1059. 4

Valencia R, Valls Miro J, Dissanayake G and Andrade-Cetto J (2012) Active Pose SLAM. In: *Proc. IEEE/RSJ Int. Conf. Intell. Robots Syst.* pp. 1885–1891. 34

Van Den Berg J, Abbeel P and Goldberg K (2011) LQG-MP: Optimized path planning for robots with motion uncertainty and imperfect state information. *The Int. J. Robot. Res.* 30(7): 895–913. 4

Von Mises R (1964) *Mathematical theory of probability and statistics*. Academic Press. 6

Yamauchi B (1997) A frontier-based approach for autonomous exploration. In: *Int. Sym. Comput. Intell. Robot. Automat.* pp. 146–151. 3

Yu J, Karaman S and Rus D (2015) Persistent monitoring of events with stochastic arrivals at multiple stations. *IEEE Trans. Robot.* 31(3): 521–535. 3